Rafael Guarino Soutelino

On the dynamics of the Brazil Current site of origin

Corrected Version

Presented as partial fulfillment of the requirements for the degree of Doctor of Philosophy in Oceanography at the Instituto Oceanográfico da Universidade de São Paulo, with emphasis in Physical Oceanography.

Adviser:
Prof. Dr. Ilson Carlos Almeida da Silveira
University of São Paulo
Co-Adviser:
Prof. Dr. Avijit Gangopadhyay
University of Massachusetts at Dartmouth

São Paulo
2012

UNIVERSIDADE DE SÃO PAULO
INSTITUTO OCEANOGRÁFICO

On the dynamics of the Brazil Current site of origin

Corrected Version

Rafael Guarino Soutelino

Presented as partial fulfillment of the requirements for the degree of Doctor of Philosophy in Oceanography at the Instituto Oceanográfico da Universidade de São Paulo, with emphasis in Physical Oceanography.

Evaluated in _____ /_____ /_____

Prof. Dr.	Grade
Prof. Dr.	Grade
Prof. Dr.	Grade
Prof. Dr.	Grade
Prof. Dr.	Grade

"The greatness of a man is not in how much wealth he acquires, but in his integrity and his ability to affect those around him positively"

Robert Nesta Marley

Contents

Acknowledgements

The factors that contribute to formation of a PhD student and culminate on this dissertation are so extensive and extends so much further than the academic world that would be impossible and unfair to write one or two pages of acknowledgments. I'll try my best though, and apologize if I leave something behind.

I first acknowledge my family for providing me stability to totally focus on my studies, to model my values and to help me understand and face mine and world's imperfections with wisdom and patience. Thanks to my family and friends to understand my physical and emotional absence and ups and downs associated with the graduation years.

Endless thanks to the restless support I got from Juliana all these years. She was the most patient one, taking all the heat of my PhD student life caveats. I can't forget about her family, amazing folks that were always there for me, thrusting and providing excellent quality leisure family time when was most needed at São Paulo.

I thank all the professors that interacted with me during the courses, talks and meetings, for sharing their experiences. I thank all my graduation and under-graduation colleagues and friends for the amazing academic atmosphere during all these years.

I thank my advisor Ilson da Silveira for teaching me valuable disciplines, not limited only to academic, but extended to life experiences and ethics. I owe to him much gratitude for the education, background and success I have as a scientist and oceanographer. Thanks for all the opportunities and transmission of confidence. My time in Ilson's lab is the ground basis of what I am as a scientist and it will always be a sure place to seek guidance, advice and partnerships.

I'm grateful for the amazing working environment provided in IOUSP, for its pro-

fessors, faculty, technicians and all for the usual qualification, seriousness and efficiency.

I also thank my co-advisor Avijit Gangopadhyay for making a major contribution to my skills as a numerical modeler and scientist and for providing a very productive, comfortable and professional atmosphere during my time in USA.

I owe many thanks to several colleagues that helped me on discussions about my work, related research and PhD student general difficulties, but I specially remember Andre Schimidt, Paulo Henrique Calil, Cayo Franciso, Ayan Chauduri, Gustavo Mastrorocco, Georgia Kakoulaki, Mithun Mullick, Jianfeng Wang, Marco Pedulli, Susan, Frank Smith (and all the SMAST folks) Cesar Rocha, Sueli Godoi, Wellington Ceccopieri, Leandro Ponsoni, Thiago Biló, André Paloczy, Ronaldo Sato, Leilane Gonçalves, Ana Paula Krelling, Fabrício Sanguinetti, Sandro Paixão, Felipe Santos, Fernando Marin, Fabíola, Raquel Mello, Marina Viera, Rafael Gonçalves, Felipe Sarquis, Rafael Mattos, and so many others.

I thank my new colleagues and friends from IEAPM. Forming a great team, they were very supportive in the tough final phase of this dissertation, thrusting in my capabilities and understanding my absences to dedicate to the final writing. Thanks Leandro Calado, André Lobato, Victor Godoi, Gabriel Serrato, Gabriel Codato, Letícia Portella, Ana Cláudia, Simone Pacheco, Sandro Paixão, Diego Miranda, Phellipe Couto, Gava and others.

I'm grateful to the Brazilian Navy and the University of São Paulo for the observational datasets, and to the Brazilian agency CNPq for funding me during these years. OCCAM data is made available by the National Oceanography Centre at `http://http://www.noc.soton.ac.uk/JRD/OCCAM/`. I also thank Collecte Localisation Satellites Space Oceanography Division (CLS/SDO) (`http://atoll-motu.aviso.oceanobs.com/`) for the altimeter AVISO data. We also thank João Lorenzzetti (INPE, Brazil) for the drifter data, and Frank Smith (SMAST/UMassD) for his editorial assistance.

We are grateful to the Brazilian agencies CNPq and CAPES for supporting the first author and providing the unique opportunity of studying abroad. This work is part of the PROABROLHOS project. We thank SMAST and UMASSD for supporting the

first author as a visiting scholar. Thanks are also given to A. Peliz, G. Flierl, W. Arruda, R. Matano, S. Baker-Yeboah and I. Belkin, E. Van Sebille for all the suggestions and discussions.

This dissertation was entirely developed using free and open source operational system, programming language and oceanographic tools. Therefore, I acknowledge and support the developing comunities of Linux (Debian and Ubuntu), Python (modules packages and toolboxes), ROMS, CODAS, LaTeX and Inkscape. These tools are listed bellow:

http://www.linux.org
http://www.debian.org
http://www.ubuntu.com
http://www.python.org
http://www.enthought.com/products/epd_free.php
http://www.scipy.org/
http://matplotlib.org
http://pydap.org
http://code.google.com/p/python-seawater/
http://myroms.org
http://currents.soest.hawaii.edu/docs/doc/index.html
http://www.latex-project.org/
http://inkscape.org/

Agradecimentos

Os fatores que contribuem para a formação de um PhD e que culminam em sua tese são tantos, e extrapolam tanto os limites do meio puramente acadêmico que seria impossível e injusto materializar os sentimentos de gratidão em apenas uma ou duas páginas. Darei meu máximo, entretanto, já me desculpando se deixei alguma coisa para trás.

Primeiramente agradeço minha família novamente por sempre ter me garantido estabilidade financeira e emocional em todos esses anos, que se traduziram no imenso privilégio de eu poder investir tanto nos estudos. Obrigado a todos da minha família e aos amigos mais próximos por entenderem minha ausência tanto física quanto emocional, bem como os altos e baixos da vida de um pós-graduando.

Imensuráveis agradecimentos ao suporte incansável da minha Ju durante todos estes anos. Ela foi sempre a mais paciente, segurou os maiores dos estresses relacionados à escalada de um doutorando, além de estar sempre preocupada e envoldida com a própria tese. Não posso deixar de mencionar também sua família, pessoas maravilhosas que sempre me acolheram com a alegria e serenidade necessárias para amenizar as dificuldades da rotina, proporcionando momentos em família de excelente qualidade em São Paulo e imediações.

Agradeço a todos os professores que interagiram comigo durante os cursos, palestras, congressos, encontros, por dividirem suas experiências e sabedorias. Agradeço a todos os meus colegas e amigos de graduação e pós graduação pela incrível atmosfera agradável por eles proporcionada durante estes anos.

Agradeço ao meu orientador Ilson da Silvera por me ensinar conceitos valiosos, não apenas acadêmicos mas extendidos a experiencias de vida e ética. Eu devo ele muito

de minha educação e sucesso como oceanógrafo e cientísta. Obrigado por todas as oportunidades e confiança em mim depositada. Meu tempo no laboratório do Ilson é a fundação do que sou hoje como cientista e sempre será um lugar seguro para procurar conselhos e parcerias.

Sou grato ao IOUSP pela excelente atmosfera de trabalho, por seus professores, técnicos e funcionários, pela competência e seriedade sempre exercidas.

Agradeço também ao meu co-orientador, Avijit Gangopadhyay por oferecer grandes contribuições para aprimorar minhas habilidades de modelista numérico e cientista, e por proporcionar-me um ambiente de trabalho bastante produtivo, calmo, confortável e profissional durante minha estada nos EUA.

Devo agradecimentos a muitos amigos e colegas que me ajudaram em discussões sobre meu trabalho, outros correlatos e dificuldades gerais da vida de um aluno de doutorado. Especialmente, cito Andre Schimidt, Georgia Kakoulaki, Mithun Mullick, Jianfeng Wang, Marco Pedulli, Susan, Frank Smith (e todos os amigos da SMAST-UMASSD) Cesar Rocha, Sueli Godoi, Wellington Ceccopieri, Leandro Ponsoni, Thiago Biló, André Paloczy, Ronaldo Sato, Leilane Gonçalves, Ana Paula Krelling, Fabrício Sanguinetti, Sandro Paixão, Felipe Santos, Fernando Marin, Fabíola, Raquel Mello, Marina Viera, Rafael Gonçalves, Felipe Sarquis, Rafael Mattos, e muitos outros.

Agradeço a meus novos amigos e colegas do IEAPM. Compondo uma grande equipe, eles sempre me ofereceram suporte na fase final do doutorado, confiando em minhas capacidades e entendendo minhas ausências para me dedicar ao texto final. Obrigado Leandro Calado, André Lobato, Victor Godoi, Gabriel Serrato, Gabriel Codato, Letícia Portella, Ana Cláudia, Simone Pacheco, Sandro Paixão, Diego Miranda, Phellipe Couto, Gava e outros.

Sou grato a Marinha do Brasil e à Universidade de São Paulo pelos conjuntos de dados observacionais e a agência de fomento CNPq por dar suporte financeiro. Agradeço ao National Oceanography Centre e ao Collecte Localisation Satellites Space Oceanography Division (CLS/SDO) pelos dados do modelo OCCAM e de altimetria AVISO, respectivamente. Agradeço também ao Dr. João Lorenzzetti (INPE, Brazil) pelos dados de derivadores e Frank Smith (SMAST/UMassD) pela assitência editorial.

Sou grato as agências de fomento CAPES e CNPq pelo suporte e por propicia-

rem a experência ímpar de se estudar no exterior. Este trabalho é parte do projeto PROABROLHOS. Agradeço à SMAST and UMASSD pelo suporte como pesquisador visitante. Também agradeço aos pesquisadores A. Peliz, G. Flierl, W. Arruda, R. Matano, S. Baker-Yeboah and I. Belkin, E. Van Sebille por todas as sugestões e discussões científicas.

Esta tese foi completamente desenvolvida com ferramentas computacionais gratuítas e de código livre, como o sistema operacional, linguagem de programação e ferramentas oceanográficas. Portanto, agradeço a apóio as comunidades de desenvolvedores do Linux (Debian e Ubuntu), Python (e seus módulos, pacotes e ferramentas), ROMS, CODAS, LaTeX e Inkscape. Vide URLs abaixo:

http://www.linux.org
http://www.debian.org
http://www.ubuntu.com
http://www.python.org
http://www.enthought.com/products/epd_free.php
http://www.scipy.org/
http://matplotlib.org
http://pydap.org
http://code.google.com/p/python-seawater/
http://myroms.org
http://currents.soest.hawaii.edu/docs/doc/index.html
http://www.latex-project.org/
http://inkscape.org/

Abstract

This dissertation addresses the mesoscale dynamics of the western boundary current system off Brazilian coast easternmost portion (10°-20° S). This is the area where the South Equatorial Current (SEC) of the Atlantic Ocean bifurcates, in the scope of the large scale wind driven subtropical gyre. This bifurcation, summed to the Equatorial circulation, has a complex tri-dimensional structure that leads to the formation of several different western boundary currents (WBCs) flowing in different directions and in different depths off the entire Brazilian coast. This system have been recognized to have major scientific importance in the last few years, because it is embedded in the South Atlantic Meridional Overturning Circulation (SAMOC) large scale pathways. Inter-hemisphere volume and heat net transports in different depths are partly controlled by the time-averaged effect of mesoscale features occurring in the region cited above, being these generated locally or remotely. This dissertation intends to address the upper ocean regional dynamics of this area in two self-contained chapters. Each of these chapters can stand alone, independently describing the problem, the methods, the results, and their implications. The contents of each chapter are summarized in the next paragraphs.

The Brazil Current (BC) originates with the arrival and bifurcation of the southernmost branch of the South Equatorial Current (sSEC) at the surface between 10-20°. The BC is a surface-cored feature and it transports warm and salty waters poleward. Previous climatological studies showed a stratified sSEC bifurcation and that the resulting southern branch formed a shallow BC - a weak western boundary current. The site of origin of the BC is currently one of the less explored aspects of regional circulation and mesoscale activity in the South Atlantic Subtropical gyre westernmost portion. Chapter 1 of this work aims to fill this gap in the 10°-20°S zone off the Brazilian coast.

The analysis of three recent synoptic surveys and global model outputs challenge the description of a continuous BC. According to our analysis, The sSEC bifurcation signal near the continental margin is unclear, and the velocity fields are dominated by mesoscale eddies. Recurrent anticyclones that seem to be related to the meandering BC leads us to construct a picture of a flow strongly influenced by topography and probably very unstable. Given this new emerging scenario, we hypothesize that the Brazil Current is eddy-dominated to the north of 20°S.

Chapter 2 of this dissertation assumes the hypothesis formulated in Chapter 1 to be true, and studies the roles of vertical shear and topography on the eddy formation near the site of origin of the BC. We present numerical simulations that show that the main realistic mesoscale features in the eddy-rich vicinities of the BC site of origin can be successfully modeled through the dynamical interaction between parameterized versions of two opposing mean western boundary currents (BC and North Brazil Undercurrent - NBUC) and local topography, with no influence of remote dynamics or atmospheric forcing. Three large BC-related anticyclones described in Chapter 1 are reproduced and present a steady behavior during one year run. Two additional sensitivity experiments are performed. When NBUC is removed from the physical context, BC interaction with topography is not sufficient to generate such eddies, and the overall pattern shows considerably less resemblance with real data. When an idealized flat-bottom and no-banks topography is considered, BC-NBUC interaction is also not capable of developing realistic mesoscale structures. Our analyses suggest that leeward anticyclonic eddy generation mechanism is occurring at NBUC vertical levels (around 400 m) at the lee of bathymetric promontories and that this is driving the appearance of these eddies in the surface levels (BC domain) with a 10 days time lag.

This dissertation structure is based on two existing scientific papers, both having the current PhD candidate as the first author, and co-authorship of his advisor, co-advisor and colleagues. Chapter 1 refers to the results of an article published at the *Geophysical Research Letters* scientific journal [*Soutelino et al.*, 2011] and the Chapter 2 refers to an article currently submitted to *Continental Shelf Research* [*Soutelino et al.*, subm]. The contents of both Chapter 1 and Chapter 2 are expanded in respect to the publica-

tion versions. More details regarding the applied methods and additional graphics and computations are shown. Finally, Chapter 3 ends the dissertation with final remarks.

Resumo

O objetivo desta tese é estudar a dinâmica de mesoescala do sistema de correntes de contorno oeste ao largo da costa leste brasileira entre 10°-20° S. Esta é a área em que a Corrente Sul Equatorial (CSE) se bifurca, no escopo da circulação de larga escala forçada pelo vento associado ao giro subtropical do Atlântico Sul. Este sistema de bifurcação, somado à circulação equatorial, tem uma estrutura tri-dimensional complexa que implica na formação de diversas correntes de contorno oeste (CCOs) que fluem ao largo da costa brasileira. Este sistema de CCOs tem sido reconhecido na literatura como de extrema importância nos últimos anos, por estar embebido nos padrões de larga escala da Célula de Revolvimento Meridional no Atlântico Sul. Transportes de calor e volume entre hemisférios em diferentes profundidades são parcialmente controlados pela média de longo termo da atividade de mesoescala na região supracitada, seja esta gerada localmente ou forçada remotamente. Esta tese objetiva estudar a dinâmica do oceano superior nesta região em dois capítulos idependentes. Cada um destes capítulos são auto-suficientes em seu conteúdo, descrevendo suas hipóteses, metodologia, resultados, discussões e implicações. O conteúdo de cada um destes capítulos é sumarizado nos parágrafos seguintes.

A Corrente do Brasil (CB) se origina com a chegada e bifurcação da CSE em superfície, entre 10-20°. A CB é uma CCO centrada em superfície e transporta águas quentes e salinas em direção ao pólo sul. Estudos climatológicos prévios descrevem a bifurcação da CSE como um fenômeno estratificado vertical e horizontalmente, e que o ramo sul da CSE dá origem a CB - uma corrente de contorno oeste fraca e rasa. A origem da CB é atualmente um dos aspectos menos explorados da circulação regional e sua atividade de mesoescala na parte oeste do giro subtropical do Atlântico Sul. O Capítulo 1 deste trabalho objetiva preencher esta lacuna de conhecimento des-

critivo na porção entre 10°-20°S ao largo da costa brasileira. A análise de três cruzeiros quase-sinóticos recentes em conjunto com padrões inferidos por altimetria e modelos de circulação global, confronta a descrição da CB como uma corrente de contorno oeste contínua. De acordo com nossas análises, o sinal da bifurcação da CSE próximo à costa não é claro, e os campos de velocidade são dominados por estruturas vorticais de mesoescala. Anticiclones recorrentes que aparentam estar associados ao meandramento da CB, nos conduzem a estabelecer um cenário de escoamento fortemente influenciado pela topografia e possivelmente instável. Diante desde cenário, sugerimos que a CB se caracteriza por um escoamento dominado por vórtices ao norte do paralelo de 20°S.

O Capítulo 2 parte do pressuposto enunciado no Capítulo 1 e objetiva estudar os papéis do cisalhamento vertical e da topografia na formação dos vórtices observados na região de origem da CB. Apresentamos simulações numéricas de estudo de processo que mostram que as principais feições realísticas de mesoescala nas imediações da origem da CB podem ser reproduzidas com sucesso a partir da interação dinâmica entre versões parametrizadas do escoamento médio de dois jatos de contorno oeste fluindo em sentido oposto (CB e Sub-corrente Norte do Brasil - SNB) e a topografia local, sem influência de dinâmca remota ou forçantes atmosféricas. Três extensos anticiclones reportados no Capítulo 1 são reproduzidos e apresentam um comportamento estacionário durante um ano de simulação. Dois experimentos de sensitividade adicionais são conduzidos. Quando a SNB é suprimida do contexto físico, a interação entre CB e topografia não é suficiente para reproduzir tais feições anticiclônicas, e em geral, o padrão obtido exibe pouca semelhança aos dados observacionais. Quando uma topografia idealizada, livre de bancos e montes submarinos é adotada, a interação BC-NBUC é também insuficiente para produzir as estruturas realísticas de mesoescala. Nossa análise sugere que vórtices anticlônicos de borda de promontório ocorrem nos níveis verticais da SNB (cerca de 400 m) e que estes estão forçando o aparecimento de anticiclones em superfície (CB) cerca de 10 dias depois.

Esta tese tem estrutura baseada em dois artigos científicos pré-existentes, ambos de autoria do presente aluno, com co-autoria de seu orientador, co-orientador e colegas.

O Capítulo 1 destina-se aos resultados de um artigo publicado no periódico científico denominado *Geophysical Research Letters* [*Soutelino et al.*, 2011] e o Capítulo 2 refere-se a um artigo atualmente submetido ao periódico científico denominado *Continental Shelf Research* [*Soutelino et al.*, subm]. O conteúdo de ambos os capítulos estão expandidos em relação às versões originais para permitir maior nível de detalhamento das diversas partes que compõem o trabalho. Mais detalhes relativos às técnicas metodológicas são apresentados, bem como um maior número de gráficos, buscando maximizar a clareza do documento. O Capítulo 3 compila e sumariza os resultados oriundos de ambos os artigos científicos, e consequentemente desta tese, finalizando com sugestões para trabalhos futuros.

List of Figures

List of Tables

Chapter 1

Is the Brazil Current eddy-dominated to the north of 20°S?

1.1 Abstract

The Brazil Current (BC) originates with the arrival and bifurcation of the southernmost branch of the South Equatorial Current (sSEC) between 10-20°S. Previous climatological studies showed a stratified sSEC bifurcation and that the resulting southern branch formed a shallow BC - a weak western boundary current. The analysis of three recent synoptic surveys and global model outputs challenge the description of a continuous BC. The sSEC bifurcation signal near the continental margin was unclear in the analyses, and the velocity fields were dominated by mesoscale eddies. Recurrent anticyclones that seemed to be related to the meandering BC led us to construct a picture of a flow strongly influenced by topography and probably very unstable. Given this new emerging scenario, we hypothesize that the Brazil Current is eddy-dominated to the north of 20°S.

1.2 Introduction

The Brazil Current (BC) is the western boundary current that closes the South Atlantic Subtropical Gyre and originates at the surface bifurcation of the southernmost branch of the South Equatorial Current (sSEC) [*Reid*, 1989; *Stramma*, 1991; *Stramma & England*, 1999; *Rodrigues et al.*, 2007]. As presented in the literature to date, the description of the site of origin of the BC consists mostly of large-scale patterns based on baroclinic geostrophic estimates computed from temperature-salinity climatology. These large-scale circulation patterns (Figure 1.1) indicate that the annual climatological mean latitudinal position for the near-surface flow is between 14.5°S and 16°S [*Stramma & England*, 1999; *Rodrigues et al.*, 2007].

Near its site of origin, the climatological BC is described as a weak, shallow current transporting largely Tropical Water (TW) southward. *Peterson & Stramma* [1991] proposed an explanation for the BC low-volume transport (of about 4 Sv; 1 Sv= 10^6 m^3 s^{-1}), namely, that the bulk of the impinging southern SEC branch enters the North Brazil Undercurrent (NBUC).

For the surface latitudinal position of the sSEC bifurcation, *Rodrigues et al.* [2007] presented an annual cycle in which the bifurcation axis migrates from 10°S in November to 14°S in July. In all monthly scenarios, the surface bifurcation for the upper 200 m is very well defined and shows a BC flowing southward as a continuous stream. Dynamically, according to those authors, the seasonal variability of the sSEC bifurcation is related primarily to variations in wind forcing via combined effects of Ekman pumping and remotely forced planetary waves.

While the climatological and seasonal patterns at the BC site of origin have been investigated, the same cannot be said about the synoptic, intra-seasonal time scales. There is virtually no information on the BC organization and mesoscale activity within the 14°S-20°S latitude range. Two exceptions are the works by *Miranda & Castro* [1981] and *Stramma et al.* [1990] (Figure 1.2). The former used a quasi-synoptic hydrographic section at 19°S to describe the BC, employing the classical geostrophic method (relative to an average reference depth of 500 m). Maximum velocities of 0.72 m s^{-1} were estimated at the surface.

Stramma et al. [1990] also computed quasi-synoptic geostrophic velocity distribu-

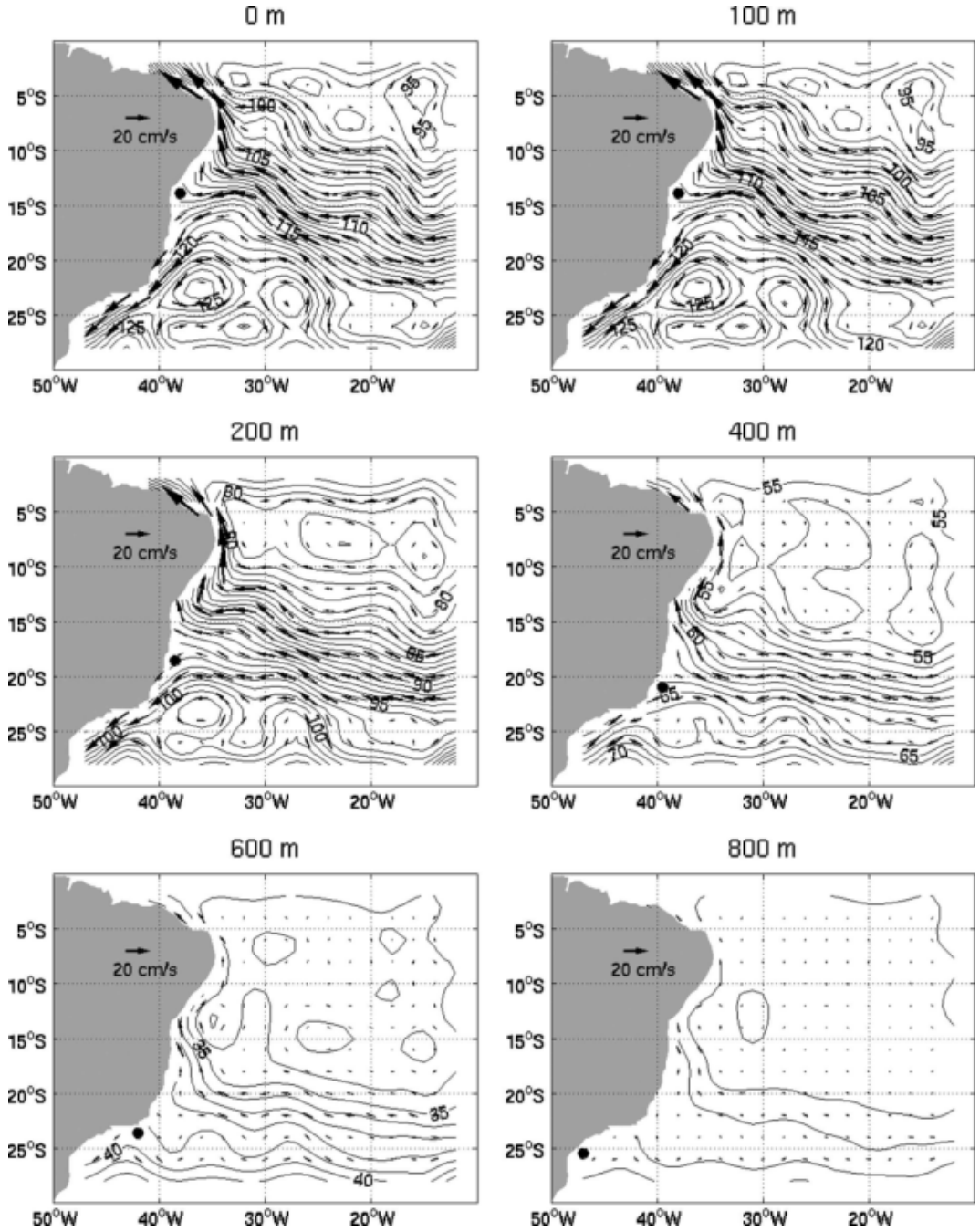

Figure 1.1: Annually averaged geopotential anomaly (x 10^{-1} m^2 s^{-2}) and geostrophic flow relative to 1000 dbar at 0, 100, 200, 400, 600 and 800 m in South Atlantic according to *Rodrigues et al.* [2007]. The black circles roughly indicates the position of the SEC bifurcation.

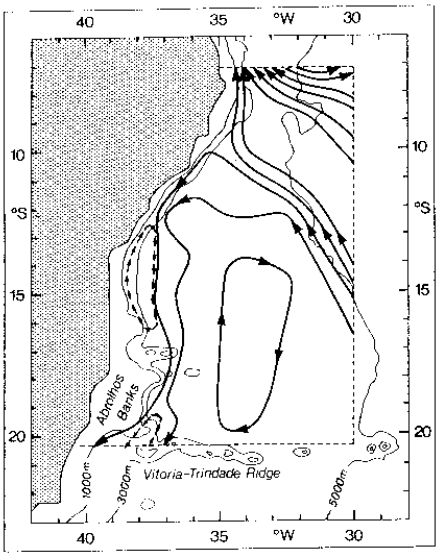

Figure 1.2: Schematic representation of time-averaged geostrophic flow based on relative velocities derived from historical hydrographic data, according to *Stramma et al.* [1990].

tions, in this case from several historical hydrographic transects off the eastern Brazilian coast between 7°S and 20°S. A section sampled in austral summer (February-March) revealed a southward-flowing BC. The authors also state that the BC does not seem to strengthen appreciably from its site of origin to 20°S. They also constructed a horizontal pattern for the BC site of origin, with the only feeding source being the bifurcated sSEC. A large cyclonic feature extending from 14°S to nearly 20°S and centered at 34°W was presented in their schema, and apparently is not connected to the BC.

The weakness of the BC flow and the convoluted shape of the continental margin with the presence of the Royal-Charlotte and Abrolhos Banks (hereafter called RCB and AbB) as well as the Vitória-Trindade Ridge (VTR) may lead to strong interaction between flow and topography. Also, the impinging of the sSEC branch in the vicinity of the Ilhéus Bight (IB) may produce a synoptic scenario that greatly differs from the climatological one.

The main objective of the present study is to build a regional synoptic picture of the origin, formation and organization of the BC as a boundary current, as well as of the mesoscale activity between 10-20°S. Recent synoptic datasets are first analyzed and simulations from an eddy-resolving ocean general circulation model (OGCM) are then presented to support the data analysis.

1.3 Satellite altimeter-derived patterns

Considering that the majority of the research done in the subject was based on climatological historical termohaline data, one would be tempted to investigate high resolution satellite altimeter-derived geostrophic velocities before looking at *in situ* synoptic datasets. Tracers climatologies like World Ocean Atlas (WOA, *Boyer et al.* [2005]) lacks spatial and temporal coverage and fail to resolve dominant flows in some areas. Recent satellite-derived sea surface height measurements allow for a more accurate estimate of the basin scale depth-averaged mean circulation. To our knowledge, no investigation based in satellite data was done in this degree of detail for the area of interest. These kind of data are highly valuable, free of cost, and despite it reflects only surface or depth-averaged quantities, it could still give interesting insights about the general behavior of the flow.

The chosen satellite altimeter product for this analysis is the AVISO - *Archiving, Validation and Interpretation of Satellite Oceanographic data* (`http://atoll-motu.aviso.oceanobs.com/`), compiled by the Collecte Localisation Satellites Space Oceanography Division (CLS/SDO). The dataset used ranges from January 1993 to July 2009. The estimation of the ocean mean dynamic topography is a combination of altimetric data, in situ measurements and GRACE geoid [*Rio et al.*, 2005]. This dataset is result of multi-satellite altimetry with 7-day temporal resolution and 1/3° longitude Mercator resolution grid. It is a blended interpolation between different altimetry sensors, made available in an equally-spaced grid map. It consists of absolute sea surface height (SSH). The spatial and temporal resolution are worse than the single altimeter data, but are adequate to map mesoscale structures, as already done by previous research.

Figure 1.3 compares, for instance, the annual long-term mean absolute geostrophic velocities determined from AVISO with the WOA-derived relative geostrophic ones. Both velocity fields were estimated using standard geostrophic relations, being the later relative to 1000 dbar, following *Rodrigues et al.* [2007]. The general flow is fairly similar between the two analysis, although some small but significant differences observed at the site of origin of the BC require attention. In the WOA-derived field (Figure 1.3a), parts of the westward SEC bend southward near Salvador, which form a continuous climatological western boundary current (14-21°S). In the AVISO-derived

flow field this southward flow is non-existent (see inner box of Figure 1.3b and Figure 1.4). This could be due to the better temporal and spatial coverage of AVISO, which resolves existing eddy activity in the region resulting in a weak mean flow without a preferred direction.

In Figure 1.4, we show more AVISO-based evidences of weak and non-organized flow in the region of interest. A zoom from the mean velocity field shows absence of magnitudes higher than 10 cm s^{-1} next to the continental margin between 12-21°S. Considering the time average of vectorial fields, this could be explained either by persistent weak velocities or any range of velocity magnitude that are inverting its direction in respect to time.

In order to explore this in more detail, the right panel of Figure 1.4 shows the time series of the along slope velocity component in two different spots, between 2007 and 2009 as an example. One spot is located within the 12-21°S (18°S, off Abrolhos Bank) range and the other is located further south, where the average flow is stronger and the BC is widely reported to have typical WBC characteristics (22°S, off Cabo Frio, *Silveira et al.* [2000b]). Note that off Abrolhos Bank, the along slope flow is indeed changing between northward and southward orientation quite a lot during the two year coverage. The flow is southward in 63% of the time, which may be a small enough percentage to consider that it has no preferred direction in this area. Off Cabo Frio, the scenario is different. As we can note, most of the time the flow is towards southwest (89 %) in this case, with a substantially higher mean magnitude (10 cm s^{-1}) compared to Abrolhos Bank region. This pattern could be related to a meandering BC, which has a mean along slope flow and recurrent perturbations associated with mesoscale eddies.

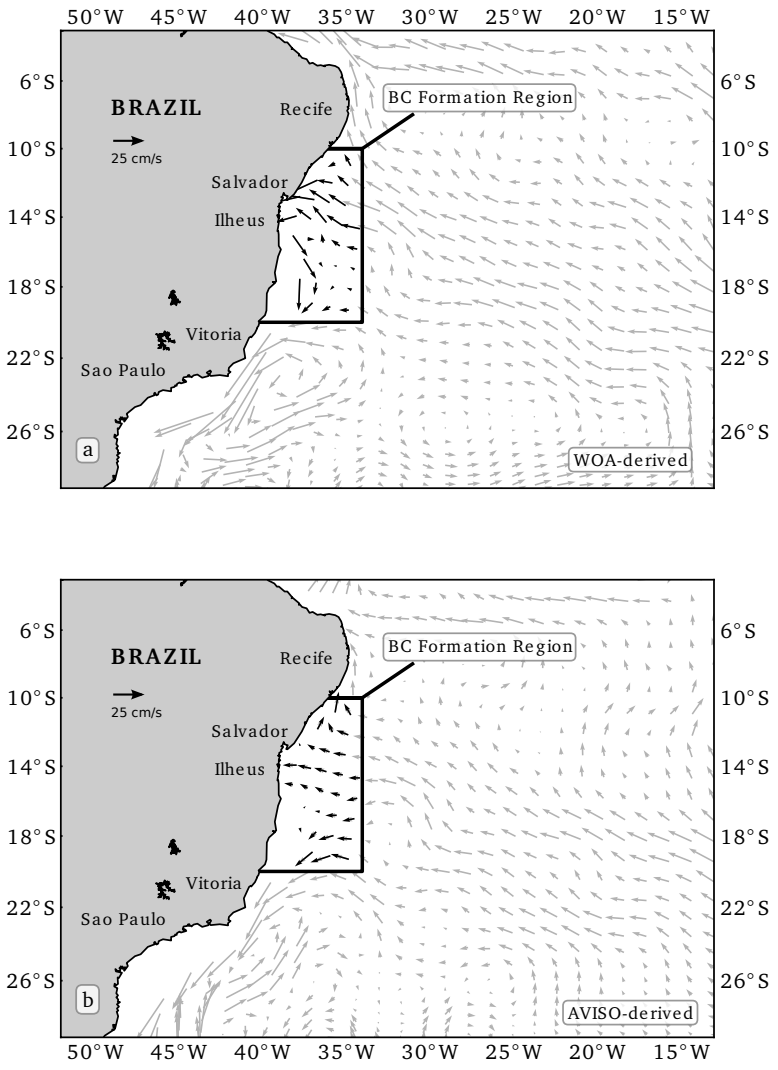

Figure 1.3: Upper panel: Annual T-S-derived streamfuction map of the South Atlantic Subtropical Gyre region at 50 m relative to 1000 m calculated from the *Boyer et al.* [2005] climatology. This map was obtained using an objective analysis scheme with a Gaussian correlation function and a decorrelation length of 470 km. The gray mask represents depths shallower than 1000 m. Lower panel: Annual long-term mean AVISO-derived geostrophic velocities.

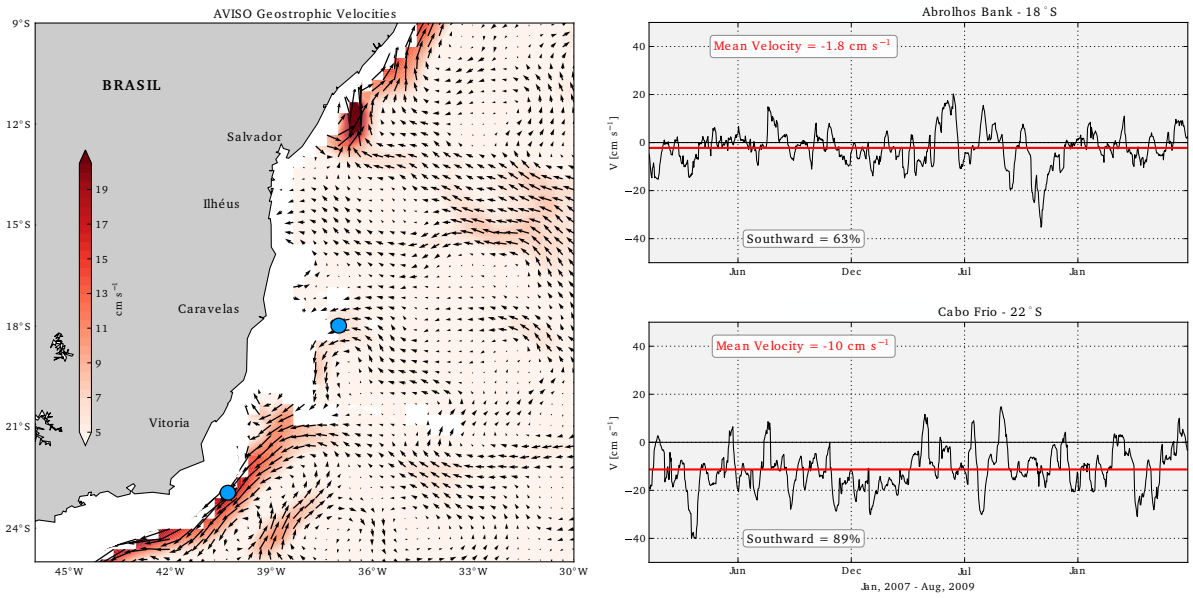

Figure 1.4: Depth-averaged AVISO-derived geostrophic velocities. Left panel: Map of long-term mean velocity field. Velocity magnitudes higher than 10 cm s^{-1} are gradually emphasized by red shades. Note the absence of these magnitudes near the continental margin between 12-21°S. The white mask adjacent to the coast represents areas shallower than 1000 m, where the altimeter lacks accuracy. Right panels: 2007-2009 along-shore velocity time series in two different locations, identified by the blue circles at the left panel.

1.4 *In Situ* data-derived patterns

1.4.1 Datasets description

Three synoptic oceanographic cruises were available as valuable *in situ* observational datasets to be used in this research, and they are summarized in Table 1.1. Detailed description of each survey will follow up in this section.

Table 1.1: Summary of the *In Situ* oceanographic cruises used in this work.

Name	Date	Institution	Data type
Oceano Leste I	Nov/2001	Brazilian Navy	CTD
Oceano Leste II	Mar/2005	Brazilian Navy	ADCP
PRO-ABROLHOS	Sep/2007	University of São Paulo	ADCP, surface drifter

The Oceano Leste I (OEI) cruise was conducted by the Brazilian Navy between 01 November and 15 December 2001. The data set consisted of top-to-bottom Seabird SBE 9Plus CTD measurements, within the domain represented in Figure 1.5a. Geostrophic velocities were calculated relative to the average depth of the σ_θ = 26.8 kg m^{-3} surface ($\approx$ 1200 m), as suggested by *Silveira et al.* [1994]. Horizontal distributions of geostrophic velocities were obtained via objective analysis mapping, as detailed in Section 1.4.2.

The Oceano Leste II (OEII) cruise was conducted by the R/V *Antares* (Brazilian Navy) between 01 February and 12 March 2005. The data set made available to us consisted of 75 kHz RD Instruments shipboard ADCP transects within the same sample area of OEI CTD cruise (Figure 1.5b). The ADCP was linked to a differential global positioning system and a scientific gyroscopic compass as heading source. The raw velocity data was collected using a vertical bin height of 8 m, with the first reliable bin representing a velocity mean from 16 to 24 m in depth. The depth penetration was about 300 m, varying according to the sea state. The data were processed and calibrated using the Common Ocean Data Access System (CODAS) [*Firing et al.*, 1995]. We applied standard calibration procedures from CODAS package to determine the orientation of the transducer relative to the gyroscopic compass, as in *Joyce* [1989] and

Pollard & Read [1989]. Horizontal distributions of horizontally non-divergent velocities were obtained via objective analysis mapping, using as input the CODAS-analyzed field, as described in the Section 1.4.2.

The third synoptic data set analyzed is the PRO-ABROLHOS shipboard ADCP cruise conducted by the R/V *Prof. W. Besnard* in the 20-30 September 2007 period. The 150 kHz RD Instruments ADCP was set up similarly to the R/V *Antares* instrument. The cruise domain is confined to the region between 17°S and 22°S (Figure 1.5). Data processing and objective mapping procedures were analogous to those described for the OEII cruise.

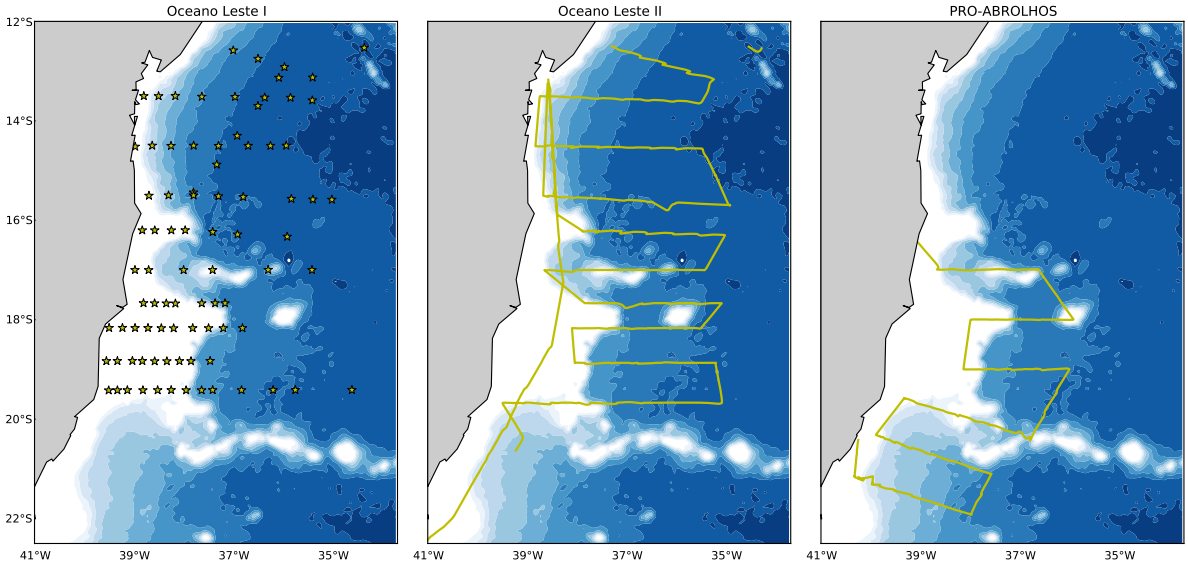

Figure 1.5: Sample area of the three *in situ* oceanographic cruises analyzed in this work. Left: OEI CTD stations. Center: OEII VM-ADCP tracks. Right: PRO-ABROLHOS VM-ADCP tracks.

1.4.2 Velocity Estimation Techniques

The dynamical assumption that is made in order to estimate the velocity fields is the geostrophic approximation, given the spatial and temporal scales of the mesoscale phenomena that we aim to study. The CTD data of the OEI cruise allows for an estimation of relative geostrophic velocities, while the ADCP direct measurements of OEII and PROABROLHOS allows for a more accurate estimation of absolute non-divergent near-geostrophic velocities. Both approaches will be detailed in the next paragraphs.

Because of the non-divergent nature of the geostrophic flow, one can represent the velocity field as a streamfunction (ψ), as in

$$u = -\frac{\partial \psi}{\partial y} \qquad ; \qquad v = \frac{\partial \psi}{\partial x}. \tag{1.1}$$

According to *Pond & Pickard* [1983], ψ in an isobaric level p can be obtained through the simple relations

$$\psi_{(p_0/p)} = \frac{\Delta\Phi}{f_0}, \tag{1.2}$$

$$\Delta\Phi = \int_{p_0}^{p} \delta_\alpha dp, \tag{1.3}$$

where $\Delta\Phi$ is the geopotential anomaly, which is totally dependent on termohaline data and reference level (p_0) of supposedly known velocities. Usually, in the absence of direct velocity measurements that could be used as reference, it is standard to use a fixed *level of no motion* as an approximation. That is the case of the OEI dataset. Therefore, using the Eqs. 1.2-1.3, one can have an estimation of geostrophic ψ in each CTD station. The *level of no motion* used here is based on *Silveira et al.* [1994] work, whom adopted the average depth of the σ_θ = 26.8 kg m^{-3} surface ($\approx$ 1200 m), because it represents the interface of two major water masses in the region (SACW and AAIW), where there is a flow reversal between two western boundary currents (NBUC and DWBC).

Once we have computed ψ for each hydrographic station, since they are sparse and irregularly distributed, we need to map these values into a regular grid before computing its spatial gradients that will finally lead to geostrophic u and v. In this interpolation process, we must be thoughtful of the temporal and spatial aliases imposed by the non-instantaneous characteristic of the dataset. The technique to perform this mapping was the *Objective Analysis* (OA). According to *Bretherton et al.* [1976], the OA of oceanic data is based in the Gauss-Markov theory, and can be thought as a least squares adjustment of the samples, where the weight function depends on the data auto-correlation behavior.

For oceanic fields, which have a fairly continuous and isotropic spatially changing behavior, it is usual to use the Gaussian 2-D correlation function

$$C(r) = (1 - \epsilon^2)e^{-r^2/l_c^2}, \tag{1.4}$$

where $r = \sqrt{x^2 + y^2}$, x and y represents the distance among stations and l_c is the horizontal length scale of the features of interest. The choice of l_c determines the degree of spatial filtering desired to the interpolation method. In the present case, $l_c \approx 100$ km was adopted, based on the gaussian fit to the auto-correlation curve of the data, in respect to spatial lags. Using this value of l_c, small ψ gradients associated with scales that are smaller than the geostrophic ones, which are not adequately resolved by the time and spatial resolution of the data acquisition, are minimized, avoiding contamination of the final field.

In the case of OEI and PROABROLHOS cruises, direct velocity measurements are available, and hence the approach is different. ADCP measurements are instantaneous samples of the fluid velocity in a given moment. The velocity measured by ADCPs retains all possible scales of motion, introducing a lot of noise to the background geostrophic flow. Therefore, what requires attention here is to avoid and/or filter ageostrophic signal of the observed velocities. According to *Sutton & Chereskin* [2002] and *Pickard & Lindstrom* [1993], there are three main sources of ageostrophic motion in oceanic regions:

- ✓ Ekman drift caused by the wind stress;
- ✓ near-inertial currents;
- ✓ tidal currents.

The first step to avoid ageostrophic signal would be the choice of a level deep enough to be out of the Ekman layer. The level chosen here is 50 m, which is a trade-off between having a perfect Ekman-free field and being shallow enough to stay within the BC core depth. According to the authors, near-inertial and tidal currents are naturally filtered during the OA process, because of its short time and spatial scales compared to the ones of the geostrophic flow.

It is worth mention that the OA scheme used for the ADCP velocities is different from the one applied to the OEI CTD data. In this case, the vectorial OA (VOA) is applied, which gets u and v from the ADCP as input and outputs observed ψ, as in *Silveira et al.* [2000a]. The principle of this technique is that a given velocity field can be described as

$$\vec{v} = (u, v) = \vec{k} \times \bigtriangledown\psi - \bigtriangledown\chi, \tag{1.5}$$

which is the sum of the velocity potential χ and the streamfunction ψ. In this case, χ is the irrotational but divergent part of the flow and ψ is the non-divergent but rotational part. The computations within the VOA scheme simply remove the χ part of the velocity field. In this process, every non-divergent movement signal that is within the sampled data is automatically removed, minimizing the ageostrophic components.

Having described the careful steps to retain the adequate velocity scales from the different nature datasets, the next section is dedicated to describe the observed mesoscale patterns.

1.4.3 Mesoscale Patterns Description

The geostrophic velocity pattern depicted from OEI is rather complex and full of eddy structures (Figure 1.6a). The sSEC bifurcation signature is not distinctive on the map. By examining the vicinity of the western boundary, we can only identify southward flow between 17°S and 20°S. Surface (relative) velocities reach 0.5 m s^{-1} in the southern part of the survey domain. This southward flow is related to two anticyclonic features centered at approximately 17.5°S and 19°S. The inspection of the whole cruise domain points to two regions of nearly westward flow entering the study area. The more southerly one is related to the upper sector of the 17.5°S anticyclone. The one to the north is also associated with another anticyclone, in this case centered at 15.5°S. Both features are near the eastern limit of the sampled area, where interpolation errors are higher. But it seems that most of the incoming flow associated with the 17.5°S anticyclone merges with the 19°S one and flows poleward along the continental margin. This eventually may represent the origin of the BC. On the other hand, the northern

15.5°S feature seems to be associated with a more closed circulation and contributes very little to the northward flow along the boundary. North of 17°S, the western border of the domain is dominated by two cyclonic features, and hence there is a net equatorward flow in this area. It seems rather difficult to associate this northward flow, which is not continuous along the boundary, with the near-surface signature of the NBUC.

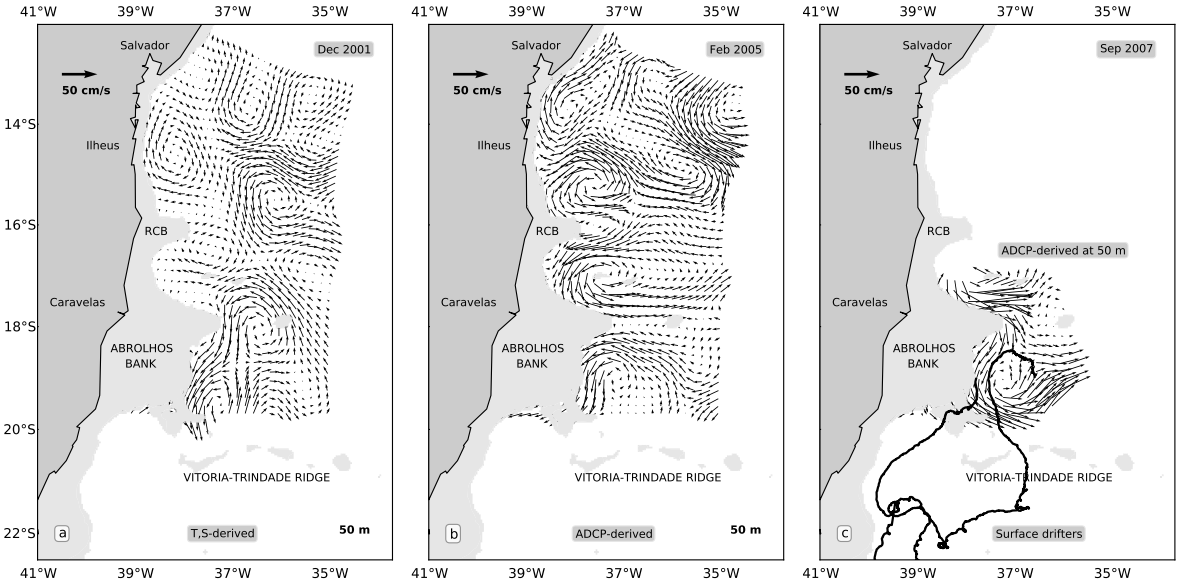

Figure 1.6: (a) T-S-derived geostrophic velocity calculated from OEI CTD data at 50 m. (b) Observed non-divergent velocities at 50 m calculated from OEII ADCP data. (c) Observed non-divergent velocities at 50 m calculated from PRO-ABROLHOS ADCP data. The black lines represent the PRO-ABROLHOS surface drifters trajectories. Vectors within the continental shelf are masked out.

As for the OEI geostrophic flow maps, we present the horizontal patterns for 50 m for the OEII. As mentioned in Section 1.4.2, we acknowledge that some Ekman drift signal, as well some other higher wavenumber phenomena, might remain in the data; however, the objective analysis interpolation procedure eliminated most of them because of (i) the horizontal non-divergence constraint of the scheme and (ii) the spatial filtering due to the decorrelation length adopted. The observed velocity field is as eddy-rich as the geostrophic velocities from November-December 2001. Velocities are also comparable in terms of magnitude between Figures 1.6a and 1.6b. In this ADCP-derived horizontal velocity pattern, we observe what could be a subtle bifurcation signature at about 15°S. To the south (north) of this latitude, the flow is dominantly

southward (northward). However, in both halves of the domain, the flow is associated with vortical structures. Three anticyclones are centered at 15°S, 17°S and 19°S, respectively. One could interpret the BC as the flow composed by the coastal border of these three features. However, the flow might or might not be continuous. The map also allows us to infer that, if there is such bifurcation, then the eddies, being the most robust structures of the field, mask its signal.

The mapped non-divergent velocity field from PRO-ABROLHOS cruise (Figure 1.6c) presents a southward flow bordering the continental margin throughout the cruise domain. This flow could be associated with the BC. Centered at 19°S, the interpolated field indicates the presence of a robust anticyclonic feature that is similar to those depicted in the OEI (Figure 1.6a) and OEII (Figure 1.6b) synoptic scenarios. In the portion of the domain north of 15°S, part of the boundary flow that contours the northern edge of the AbB moves offshore and northeastward. This might be interpreted as the southern limb of the anticyclone centered at 17°S depicted in the previous cruise analyses.

In addition to the ADCP data, two satellite-tracked surface drifters were dropped during the PRO-ABROLHOS survey. Their trajectories are presented overlain with the mapped velocities (Figure 1.6c). The drifter released at 36.75°W confirms the anticyclonic motion in the region adjacent to the AbB. However, it escapes through a gap in the VTR.

1.5 OGCM-derived patterns

In the absence of data with more temporal coverage that could enrich our findings, results from an eddy-resolving OGCM implementation are presented next (Figure 1.7) in support of the observations. The OGCM is the *Ocean Circulation and Climate Advanced Model* (OCCAM, *Webb et al.* [1998]), implemented in a domain encompassing the southern oceans, with a 1/12° horizontal resolution and 66 vertical levels. This OGCM reproduced the mean features of the general open ocean circulation off Brazil reasonably well [*Cirano et al.*, 2006]. The last year (2003) of the 14-year model run was chosen for comparing with observations. For example, compare the observed velocity fields for February 2005 (September 2007) in Figure 1.6b (1.6c) to those simulated by

OCCAM for February (September) 2003 in Figure 1.7b (1.7c).

The model simulations show neither a bifurcation signature, nor the formation of a continuous southward western boundary current, similar to observations. Eddy features are seen approximately in the same area as observed in the data sets, with recurrence of near-shelf anticyclones offshore of RCB and of AbB (Figure 1.7a and 1.7b) and also offshore Ilhéus (Figure 1.7b). Note that quantitative comparisons of the eddies regarding their strengths and sizes are not done in this study.

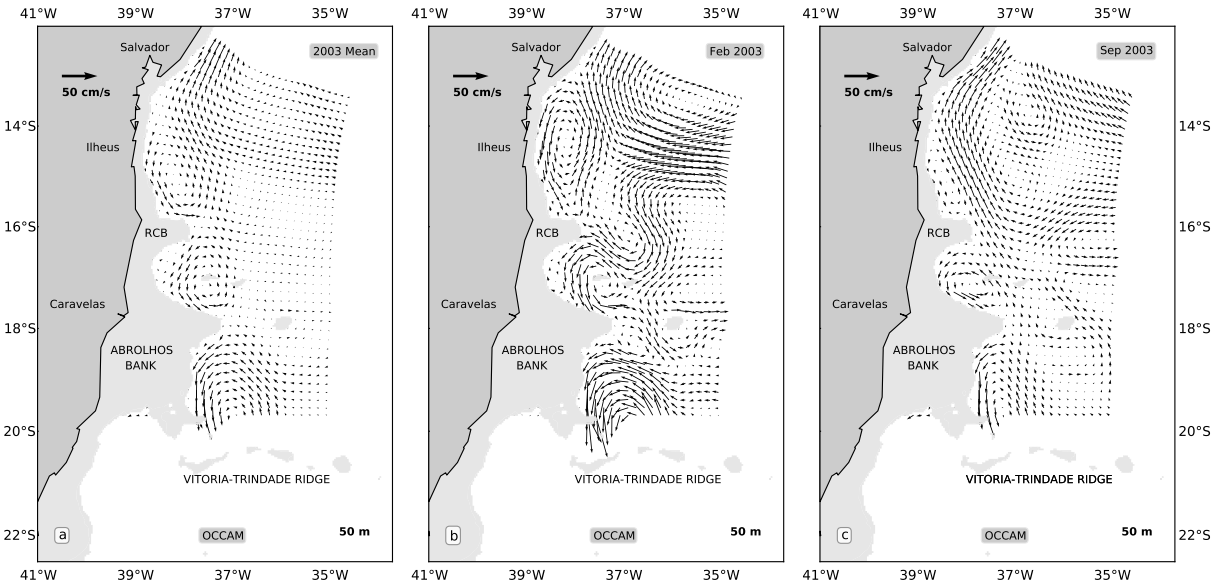

Figure 1.7: OCCAM 2003 mean velocity fields at 50 m. (a) Annual mean. (b) February mean. (c) September mean. Vectors within the continental shelf are masked out. For the sake of comparison, OCCAM velocities were interpolated to the same grid adopted to map the observed data sets.

To understand how permanent or recurrent these anticyclones are in OCCAM results, a 2003 average flow was computed (Figure 1.7a). Remarkably, the same three anticyclones can be identified from this field. We observed this three-eddy structure for most of the monthly and annual means (not shown here) of the 14-year OCCAM simulation. Note that similar eddy-dominant pattern was also observed in Southwest Indian Ocean, where the western boundary flow (Mozambique Current) is frequently broken into anticyclonic eddies in the Mozambique Channel [*Schouten et al.*, 2003]. *Biastoch & Krauss* [1999] argue that barotropic instability associated with the SEC (Indian Ocean) north of Madagascar may be responsible for its formation. In the Southwest

Atlantic, topographic features are most likely responsible for steering this eddy formation offshore the continental shelf, and also restricting what could be a continuous southward flow. Further analyses must be carried out to investigate the formation process of the BC.

1.6 Summary and Discussion

The origin of the BC is generally associated with the bifurcation of the sSEC. Climatologically, the average bifurcation axis is centered at around 15°S [*Stramma & England*, 1999; *Rodrigues et al.*, 2007]. The climatological scenario shows the northern branch feeding the upper layers of the NBUC and the southern branch originating the BC. The latter is depicted as a continuous flow that crosses the VTR and sometimes splits into two or three branches due to the ridge's zonally oriented seamounts [*Evans et al.*, 1983; *Evans & Signorini*, 1985].

The synoptic scenario revealed by satellite altimetry, three recent quasi-synoptic surveys and OGCM outputs differs from the climatological signature of the sSEC bifurcation and the BC origin. Our analysis detects no consistent pattern of bifurcation. Both observed and modeled fields are dominated by vortical features of about 100 km in radius. We analyzed different seasons, and the rich eddy field is present in all velocity distributions. South of 15°S, there is a tendency to form a southward flow that borders the continental margin and is linked to the coastal side of the anticyclones present in the area. It is not clear whether this is a continuous BC, as depicted from climatology, or simply a flow resulting from averaging a succession of counterclockwise eddy structures in the 15°S-20°S latitude range.

This intense eddy activity near the BC's site of origin has not been reported before in literature from observations. *Miranda & Castro* [1981] and *Stramma et al.* [1990], the only two previous works which dealt with synoptic data off the Brazilian east coast, presented sections of geostrophic velocity with a southward flow adjacent to the continental margin and concluded it to be the BC. The 19°S section presented in *Miranda & Castro* [1981] shows a counterflow offshore of the BC that could be compatible with a section of the anticyclone depicted in the three surveys analyzed in the present work.

Silva et al. [2009] numerically simulated the area and apparently reproduced the 19°S-centered anticyclone in their experiments, although they did not discuss the feature.

The anticyclonic eddy structures south of 15°S can be related to the convoluted form of the continental margin. The possible topographic influence on (or forcing of) the BC meanders may be similar to that which forms non-propagating meanders of the North Atlantic Current east of the Grand Banks [*Rowley*, 1996], where conservation of potential vorticity plays a crucial role.

The synoptic horizontal circulation patterns described in the present work raise a very important question regarding the formation region of the western boundary current along the eastern coast of Brazil: Is the Brazil Current north of 20°S eddy-dominated? To a first order, we suspect the answer to be yes. One might expect the cause to be either the topographical constraints on the eddies (by the AbB, VTR and RCB) or geophysical instabilities created by the BC-NBUC opposing flow system, or a combination of both.

Chapter 2

The roles of vertical shear and topography on the eddy formation near the site of origin of the Brazil Current

2.1 Abstract

The site of origin of the Brazil Current (BC) is currently one of the less explored aspects of regional circulation and mesoscale activity in the South Atlantic Subtropical gyre westernmost portion. The few studies that are available, based either on in situ data or on numerical modeling, seems to agree that the region is characterized by relatively weak and strongly baroclinic flow, with substantial mesoscale activity, which is quite different from other western boundary current systems (e.g. Gulf Stream, in the North Atlantic). We present numerical simulations that show that the main realistic mesoscale features in the eddy-rich vicinities of the BC site of origin can be successfully modeled through the dynamical interaction between parameterized versions of two opposing mean western boundary currents (BC and North Brazil Undercurrent - NBUC) and local topography, with no influence of remote dynamics or atmospheric forcing. Three large BC-related anticyclones observed in previous work were reproduced and presented a steady behavior during the run. Two additional sensitivity experiments were performed. When NBUC is removed from the physical context, BC interaction with topography is not sufficient to generate such eddies, and the overall

pattern is shows much less resemblance with real data. When an idealized flat-bottom and no-banks topography is considered, BC-NBUC interaction is also not capable of developing realistic mesoscale structures. Our analyses suggest that leeward anticyclonic eddy generation mechanism is occurring at NBUC vertical levels (around 400 m) at the lee of bathymetric promontories and that this is driving the appearance of these eddies in the surface levels (BC domain) with a 10 days time lag.

2.2 Introduction

The Brazil Current System is a vertically heterogeneous composite of layered set of western boundary currents (WBC) along the western periphery of the South Atlantic Subtropical Gyre. The surface layer, generally called the Brazil Current (BC), follows the continental shelf along eastern and southern Brazil. Its path passes over the continental shelf and slopes of several major basins – the Espírito Santo, Campos and Santos Basins – where the search for recoverable hydrocarbons is concentrated (Figure 2.1).

The vertical structure of the BC is unique among subtropical western boundary currents, in that it gets modified as the current flows southward [*Stramma & England*, 1999; *Silveira et al.*, 2004]. It is generally thought that between its site of origin (15°S) and 20°S the BC is only about 200 m deep and transports only Tropical Water (TW). South of 20°S, where the pycnocline-level South Atlantic Central Water (SACW) feeds the BC, it reaches depths of 400-500 m. At latitudes further south of 28°S, where Antarctic Intermediate Water (AAIW) is transported by the BC, the vertical extension of the current is about 1200 m [*Böebel et al.*, 1999; *Schmid et al.*, 2000] (Figure 2.1).

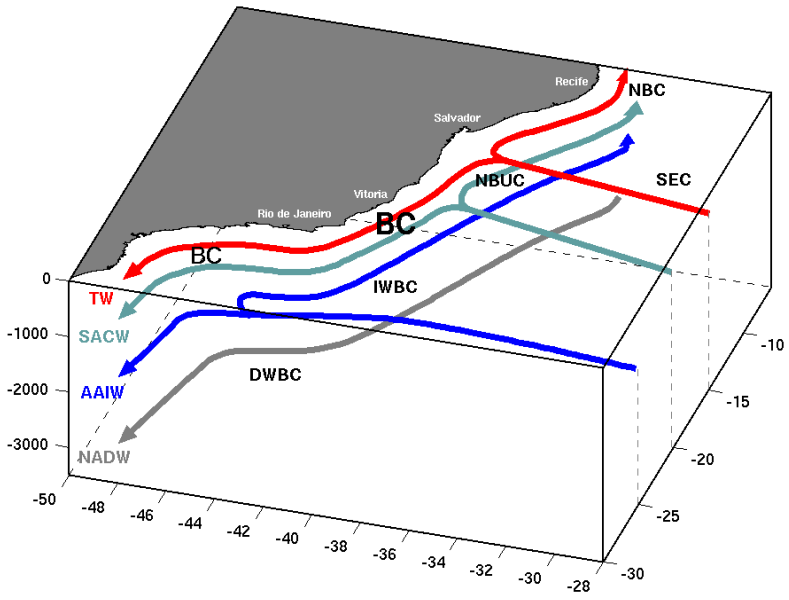

Figure 2.1: 3-D depiction of the complexity of water masses coming from different sources (which are also part of the meridional overturning circulation) to form the WBCs along the coast of Brazil.

The intricate pattern of bifurcations of the currents in the northern limb of the subtropical South Atlantic gyre is sketched in Figure 2.1. The thickening process that the BC goes through as it flows poleward is apparent. Also evident is the fact that south of 30°S, the BC and Deep Western Boundary Current (DWBC), which transports North Atlantic Deep Water (NADW), merge, and a water column of more than 3000 m flows towards the confluence region with the Malvinas Current [*Zemba*, 1991].

The annual climatological mean latitudinal position for the near-surface South Equatorial Current Bifurcation (BiSEC) is between 14.5°S and 16°S; recognized as the site of origin of the BC [*Stramma & England*, 1999; *Rodrigues et al.*, 2007] (Figure 1.1). North of the AAIW flow bifurcation (28°S), an Intermediate Western Boundary Current (IWBC) opposing the BC direction is set up. The Vitória-Trindade Ridge (VTR), a quasi-zonal seamount chain at 21°S, marks the latitude of bifurcation of the westward SACW flow [*Stramma & England*, 1999]. Therefore, north of this latitude, the SACW flows north, adding transport to the IWBC, starting a flow which becomes the North Brazil Undercurrent (NBUC) north of the SEC bifurcation. The NBUC extends from about 200 m to 1200 m [*Silveira et al.*, 1994; *Stramma et al.*, 1995; *Schott et al.*, 2005] (Figure 2.2).

The climatological description of the southward BC near its site of origin is a weak, shallow flow transporting largely Tropical Water (TW) southward. *Peterson & Stramma* [1991] proposed an explanation for the BC low-volume transport (of about 4 Sv; 1 Sv= 10^6 m^3 s^{-1}), namely, that the bulk of the impinging southern SEC branch enters the NBUC and not the BC.

There are few studies about the BC organization and mesoscale activity within the 14°S- 20°S latitude range. *Miranda & Castro* [1981] used a quasi-synoptic hydrographic section at 19°S to describe the BC, employing the classical geostrophic method (relative to an average reference depth of 500 m). Maximum velocities of 0.72 m s^{-1} were estimated at the surface.

Stramma et al. [1990] also computed quasi-synoptic geostrophic velocity distributions, in this case from several historical hydrographic transects off the eastern Brazilian coast between 7°S and 20°S. A section sampled in austral summer (February-March) revealed a southward-flowing BC. The authors also stated that the BC does not seem to strengthen appreciably from its site of origin to 20°S. They also constructed a horizontal

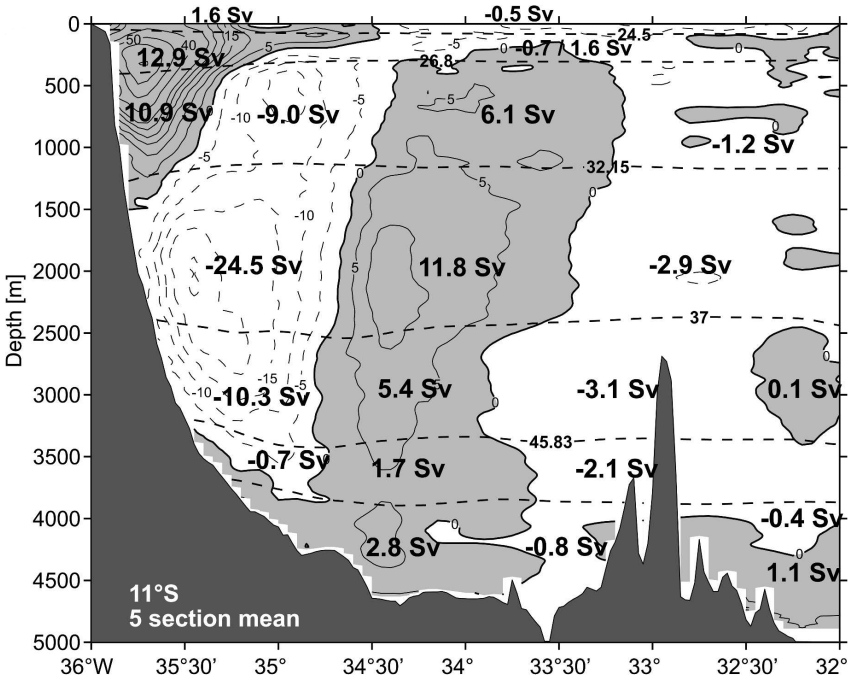

Figure 2.2: Moorings-based average sectional representation of the NBUC at 11°S, according to *Schott et al.* [2005].

pattern for the BC site of origin, with the only feeding source being the bifurcated SEC (Figure 1.2). A large cyclonic feature extending from 14°S to nearly 20°S and centered at 34°W was presented, and apparently is not connected to the BC.

Regarding mesoscale activity and eddy features present in this area, the first study, based on modeling efforts, was carried by *Campos* [2006]. The authors simulated an equatorward propagation of a cyclonic eddy feature known by the Vitória Eddy (VE). The VE was first described by *Schmid et al.* [1995] through multiple sources of observations at the lee of Abrolhos Bank (AB) (see Figure 2.3), and reported to slowly translate northeastward. *Campos* [2006] (Figure 2.4) modeled VE translational behavior described by *Schmid et al.* [1995] and noted an additional mode, where the translation continues towards the equator, crossing the Vitória-Trindade Ridge (VTR). More recently, *Arruda et al.* [subm] confirmed this translation mode through a series of satellite-derived sea surface height (SSH) maps and recent dated data-assimilative numerical experiments. Both authors discussed that the NBUC and/or interaction with other vortical feature may have a role on the advection of VE.

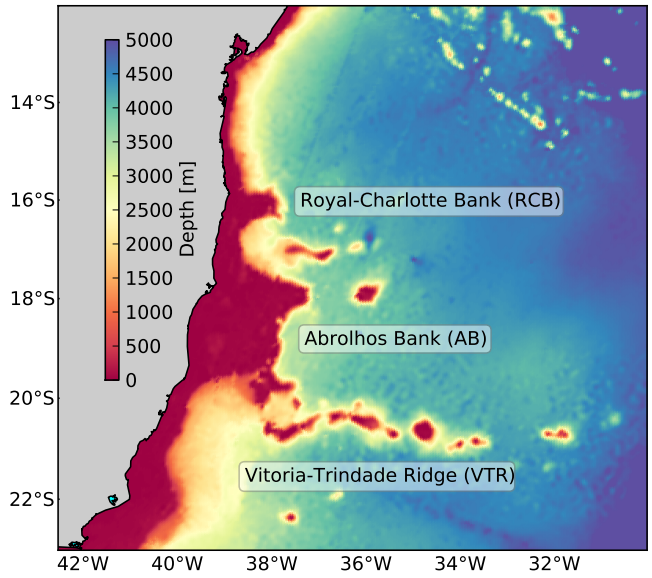

Figure 2.3: Bathymetry at the BC formation region, showing the VTR, RCB, AB and other seamounts. Source: ETOPO.

Observation-based patterns within this region were recently described by *Soutelino et al.* [2011] (Chapter 1), who analyzed three synoptic *in situ* data surveys (Figure 1.6). They reported the near-surface flow to be weak and dominated by eddies between 10°-20°S. Emphasis were brought to three persistent large anticyclonic eddies, also reproduced by the OCCAM eddy-resolving OGCM [*Webb*, 2000]. *Soutelino et al.* [2011] speculated that the eddies are either recurrent or permanent, based on their presence in annually averaged OGCM fields (Figure 1.7).

The anticyclonic eddy structures south of 15°S may be related to the complex bathymetry of the continental margin (Figure 2.3). The northernmost anticyclone is located off Ilhéus (15.5°S), the other is located north of the Royal Charlotte Bank (RCB) in the vicinity of the Ilhéus Bight, and is centered at 17°S in between the Royal Charlotte and Abrolhos Banks. The southernmost anticyclone is located offshore the Abrolhos Bank (AB) and limited to the south by the presence of the VTR [*Soutelino et al.*, 2011]. The authors raised the possibility that topographic influence on the BC meanders may be similar to that which forms non-propagating meanders of the North Atlantic Current east of the Grand Banks [*Clarke et al.*, 1980], where conservation of potential vorticity plays a crucial role.

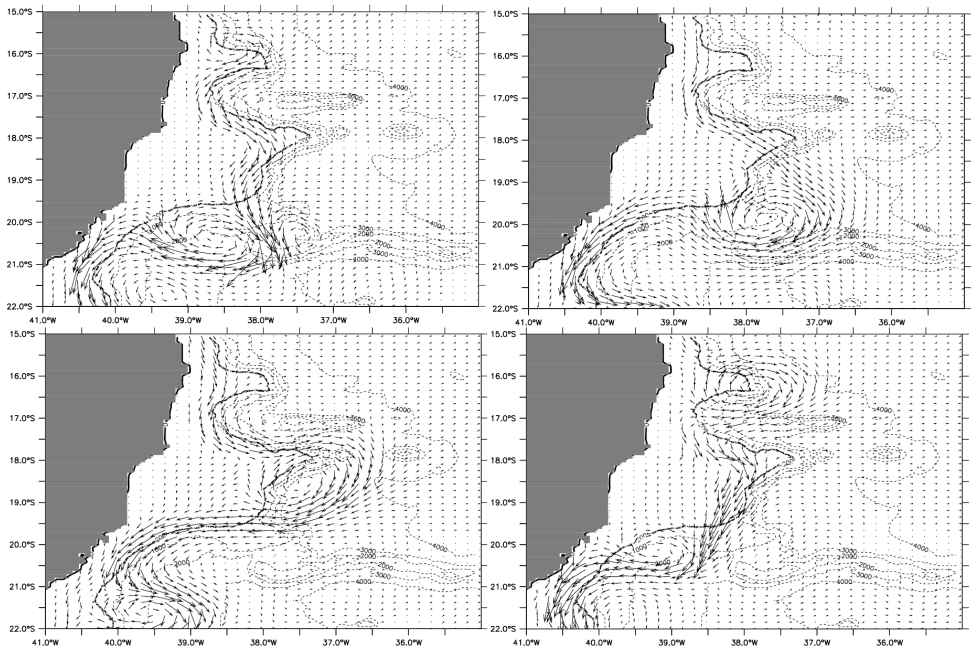

Figure 2.4: Model results illustrating the northward propagation of the Vitoria Eddy, according to *Campos* [2006].

As it is known, the BC flow is characterized by strong vertical shear with its immediate adjacent western boundary current (NBUC) of Southeast Brazil (20°-25°S). *Silveira et al.* [2008] has shown that the interaction within the baroclinically unstable BC-IWBC system further south (around 23°S) leads to the formation of mesoscale eddies. So, we believe that the existence of this unique western boundary undercurrent (NBUC) north of 20° is another possible player that favors the peculiar mesoscale activity reported by *Soutelino et al.* [2011] in our study area (Chapter 1).

According to *Verron et al.* [1991], the determination of generation, growth and decay characteristics of eddies represents a challenging problem having practical applications. The ocean region where the eddies were found represents both a preservation and conservation area due to the presence of endemic nelict coral reef species and also a future site for oil exploitation. Eddy properties can affect the local water quality and the local distribution of sediment, fauna, nutrients and chemicals [*Verron et al.*, 1991].

This work focuses on the possible roles of topography and BC-NBUC shear on the eddy activity in the near-surface flow in the BC formation region (10°-20°S), reported by the recent literature [*Campos*, 2006; *Soutelino et al.*, 2011; *Arruda et al.*, subm]. Since

there is lack of more complete and recent observational data to tackle this problem, we address it through feature oriented regional modeling process studies (FORMS - *Gangopadhyay & Robinson* [2002]). The FORMS approach consists of (i) identifying the major circulation features of the region, (ii) parameterizing such features in terms of their synoptic characteristics (u,v, t, s). (iii) implementing a dynamically balanced three-dimensional representation of the regional ocean as a nowcast, and (iv) running dynamical simulations using such 3-D initialization for nowcasting, forecasting and process studies. Details of the FORMS implementation for Eastern Brazilian Continental Margin (EBRA) region are exposed in Section 2.3. The particular parameterizations for the BC-NBUC-SEC regional setup are described in Section 2.3.1. The numerical model and design of sensitivity experiments are discussed in Section 2.3.2. The results from the CONTROL experiment (BC-NBUC with real topography) are presented in Section 2.4.1. The two velocity shear experiments (S1: BC-NBUC on flat bottom; and S2: only BC on real topography) are described in Sections 2.4.2 and 2.4.3. Section 2.5 discusses the dynamical mechanisms that could explain the eddy formation, based on quasi-geostrophic theory and energy conversions in a baroclinic instability framework. Section 2.6 concludes this work.

2.3 Parametric and Numerical Modeling Setup

According to *Gangopadhyay & Robinson* [2002], each oceanic region, however unique in their individual behavior, consists of a number of *generic* or *common* characteristic synoptic circulation structures. These synoptic entities or *features*, when put together in a particular region, interact and evolve to generate the combined circulation variability due to different regional set-up of multi-scale processes, bathymetry, boundaries and forcing due to winds and buoyancy. A regional basin like ours may include a set of multi-scale features such as large-scale meandering currents and fronts, mesoscale eddies and vortices.

This approach, called feature-oriented regional modeling system (FORMS) [*Gangopadhyay & Robinson*, 2002] consists of empirically/analytically creating initial and/or boundary conditions for momentum/tracers for primitive equation model simulations. The technique is widely used for atmospheric and ocean nowcasting and forecasting [*Robinson et al.*, 1988, 1989; *Spall & Robinson*, 1990; *Fox et al.*, 1992; *Hurlburt et al.*, 1992; *Cummings et al.*, 1997; *Gangopadhyay et al.*, 1997; *Robinson & Glen*, 1999; *Gangopadhyay et al.*, 2003; *Calado et al.*, 2008, 2010], but it is also applicable for feature-oriented process studies, as we aim here. Parameterizations of velocity features in the ocean have been widely used for theoretical studies of geophysical fluid dynamics and instabilities [*Schmidt et al.*, 2007].

According to the methodology developed by *Gangopadhyay & Robinson* [2002], when the typical characteristics of the features from previous observations or studies are known, we can parameterize them and use as input for different process studies numerical experiments and study their dynamical processes. The empirical-analytical design formulation of the three-dimensional velocity and water mass structures of a feature is called the *feature model* (FM).

We use this technique in a control experiment to analytically create the time-averaged smooth flow described mostly by *Stramma & England* [1999] and *Silveira et al.* [2000b]. We build FMs for the three currents that compose the upper 1200 m of the region limited by 10-23°S and 41-32°W (SEC, BC, NBUC). These combined features in EBRA are required to meet observation-based kinematic characteristics and mass conservation criteria. This field is then interpolated to a numerical model grid with the best available

bathymetry, and allowed to evolve for one year. This period is typically a minimum time spawn to see the development of mesoscale variability.

Thus we include (omit) each one of FMs, as well as omit(include) important topographic features in complementary sensitivity experiments, characterizing the *process-study* type of approach. Dynamical adjustment and evolution of the initial smooth velocity fields in different configurations and different bathymetry can then bring insights about the role of the different entities involved. The 3D field construction will be detailed in Section 2.3.1 as the case of the control experiment. Thorough descriptions of the sensitivity experiments will be given in Section 2.3.2.

2.3.1 An Idealized System Formulation

Velocity FMs can be designed through two main approaches [*Lozano et al.*, 1996]: forward approach and backward approach. The forward approach consists of parameterizing the shape of T and S surfaces that composes the baroclinic pressure gradients that are in geostrophic balance with the velocity structures of interest. In this case, the associated velocity field may be computed by the primitive equation model or beforehand. In the backward approach, the exact aimed velocity structure is parameterized and the thermohaline fields are computed afterwards through a variety of methods [*Gangopadhyay & Robinson*, 2002]. In this work, both velocity, T and S are considered as the initial field to the primitive equation ocean model. Generally, the choice of either approach is based on the available source of observations. Availability of direct velocity measurements favors the backward approach; and availability of thermohaline observations favors the forward approach. The velocity-based backward approach is also more suitable for current or front-dominated regions. In the present process-study work, the backward approach is employed.

In stage 1 of the FM backward approach, two quasi-meridional jets (BC and NBUC) are parameterized. In stage 2, geostrophically balanced potential temperature (T) and salinity (S) fields are computed from the FM 3D velocity field. The imposition of a NBUC flow that is intensified northward sets up a baroclinic pressure gradient. This gradient serves as forcing for a third parameterized jet - the southernmost SEC branch. Hence, stage 3 consists in computing geostrophic velocities for SEC and interpolat-

ing them to the two-jet field obtained in stage 1. The forth and last stage consists in computing the remaining prognostic variables required by the numerical model as initial conditions, which are the depth-averaged velocity field and the sea surface height (SSH). The application of each one of these stages is detailed in the following paragraphs. Starting with stage 1, BC and NBUC are both parametrized by Eq.2.1. To obtain the full three-dimensional system, we sum up Eq.2.1 fed with NBUC parameters and Eq.2.1 fed with BC parameters. The orientation of the system defined within EBRA is a natural coordinate frame of reference, where x is the cross-stream axis, y is the along stream axis and z is the vertical axis. The y axis is roughly parallel to the isobath of 150 m, which represents the interface between the coastal and the deep oceans.

The full three-dimensional main expression for both jets along-stream velocity $\mathcal{V}$ is then

$$\mathcal{V}(x,y,z) = v(y,z)\ exp\left[-\frac{(x-x_c)^2}{2\delta^2}\right], \tag{2.1}$$

which is a cross-stream Gaussian-shaped structure with a variable amplitude defined by a $v(y,z)$, which varies in the along-stream and vertical directions. For the cross-stream structure, a constant width proportional to δ is adopted for both jets, where x_c defines the position where the jet core occurs. This position x_c is also considered constant to keep the system at a fixed distance from the shelf break, roughly following the local topography. Hereinafter, the subscript c refers to *core*, which is where the maximum velocity of the jet occurs at a given y location. The subscript t refers to the top of the jet, in respect to the orientation of the z axis (upward), and b refers to the bottom portion of the jet.

For the NBUC jet, $v(y,z)$ carries its northward strengthening and shallowing velocity core, as mentioned in Section 2.2. Thus,

$$v_{NBUC} = v_c(y) \begin{cases} exp\left[-\frac{(z-z_c(y))^2}{2\delta_t^2}\right], \text{ at } z_c < z < 0 \\ \\ exp\left[-\frac{(z-z_c(y))^2}{2\delta_b^2}\right], \text{ at } z_b < z < z_c. \end{cases} \tag{2.2}$$

In Eq.2.2, v_c enables the northward strengthening and z_c represents the northward shallowing. For the sake of simplicity, both v_c and z_c increases northward as a linear function that aims to match the typical observed values of these parameters in the southern and northern limits of the domain. The vertical shear of the jet is kept constant in the along-stream axis, as an asymmetrical Gaussian-shaped structure. The upper part of the jet is less thick then the lower part, both represented respectively by δ_t and δ_b. Note that when the appropriate choice of parameters is made, this formulation enables the NBUC to reach surface at the north of EBRA, but keeps it in subsurface in the south of the domain.

In the BC case, the formulation is simpler, since there is no vertical migration of the jet core. The vertical and horizontal structure functions are the same for the NBUC. In other words, we do not need the y-dependence for the parameter z_c. Now we aim to model a jet that is surface-intensified and northward weakened in such a fashion that it completely vanishes at the approximate latitude of the BiSEC. By the time we sum both BC and NBUC, this parameterization enables a smooth transition between two different regimes: (i) the BC over the NBUC at the southern part of the domain and (ii) a surfacing NBUC with no BC at the northern part.

So, BC three-dimensional structure is parametrized by an identical Eq.2.1 with a different v formulation. As said above, the vertical structure v_{BC} now carries y-dependence only for the jet core velocity, since the jet core depth z_c is constant and at the surface, as in

$$v_{BC} = v_c(y).exp\left[-\frac{(z-z_c)^2}{2\delta_{bc}^2}\right], \ \ at \ \ z < 0. \tag{2.3}$$

Another difference regarding BC is that the surface-core jet results in only one half of the Gaussian-shaped vertical structure function, allowing us to write Eq. 2.3 as a single expression defined in $z < 0$.

The graphical representation of all the relevant FM parameters are presented in by Figure 2.5. Recall that the choice of the parameters is based literature information, where realistic jet positions, width, thickness, maximum velocities and transports are aimed. The previous works used as references for these characteristics are summarized in Table 2.1. Note that all available information is sparse in time and space and small adjustments of the parameters are allowed in order to conserve mass in the EBRA domain. The current transports were computed analytically by integrating Eq.2.1 from $-\infty$ to ∞, which results in the simple expression

$$\mathcal{T} = v_c \, \delta(\delta_t + \delta_b). \tag{2.4}$$

The parameters were chosen to reproduce the values of volume transport, core velocities, jet depth and jet width presented in the literature listed in Table 2.1. The adopted parameters are summarized in Table 2.2. Figure 2.6 illustrates the volume transport balance employed in the model boundaries of the EBRA domain, and which corresponds to the sum of eighth column of Table 2.2. Figure 2.6 is key to comprehensively illustrate the designed setup that will serve as initialization to the numerical experiments yet to be described.

Stage 2 consists in computing T and S fields by inverting the thermal wind relation and using a linearized version of the equation of state, as in *Schmidt et al.* [2007] and *Fernandes* [2007]. We use local climatological T, S and potential density (ρ) regional averaged vertical profiles to keep water masses and stratification within a realistic range. The first step to obtain T and S is to compute ρ, from the thermal wind equation

$$f_0 \frac{\partial v}{\partial z} = -\frac{g}{\bar{\rho}} \frac{\partial \rho}{\partial x}, \tag{2.5}$$

where f is the Coriolis parameter, v is interpreted as the along-shelf velocity and $\bar{\rho}$ is the reference density (1027 kg m^{-3}, from climatology). Integrating Eq. 2.5 in respect to x, we get an expression to ρ, which is

$$\rho(x, z) = \rho(0, z) - \frac{f_0 \bar{\rho}}{g} \int_0^L \frac{\partial v}{\partial z} dx, \tag{2.6}$$

where $\rho(0, z)$ is a mean density profile (also obtained from climatology) at the initial location of the transect and L is the length of the transect. Figure 2.7 show the resulting σ_θ fields computed from Figure 2.5 velocity fields. Figures 2.8 and 2.9 show how the resulting system sets horizontally, after computing all the transects in the EBRA domain.

Table 2.1: Summary of the previous work used as reference to estimate the FM geometric, kinematic and volume transport related parameters.

Feature	Relevant studies
NBUC (10°-15°S)	*Silveira et al.* [1994]
	Stramma et al. [1995]
	Stramma & Schott [1999]
	Böebel et al. [1999]
	Silveira et al. [2000b]
	Dengler et al. [2004]
	Schott et al. [2005]
	Rodrigues et al. [2007]
IWBC/NBUC (15°-25°S)	*Stramma & England* [1999]
	Böebel et al. [1999]
	Silveira et al. [2000b]
	Silveira et al. [2004]
	Rodrigues et al. [2007]
	Schmidt et al. [2007]
BC (10°-28°S)	*Stramma et al.* [1990]
	Miranda & Castro [1981]
	Silveira et al. [2000b]
	Silveira et al. [2004]
	Campos [2006]
	Rodrigues et al. [2007]
	Soutelino et al. [2011]

Table 2.2: Adopted parameters for the Velocity-based BC-NBUC FM system. See Figure 2.5 for graphical representation. Linear functions are adopted to transfer parameters from south to north, when appropriate.

Feature	x_c	δ	z_c	$\delta_t/2$	$\delta_b/2$	v_c	T
NBUC-S	160 km	100 km	500 m	100 m	360 m	20 $cm\ s^{-1}$	9 Sv
NBUC-N	160 km	100 km	200 m	100 m	360 m	50 $cm\ s^{-1}$	23 Sv
BC-S	160 km	100 km	0 m	$\times$	150 m	20 $cm\ s^{-1}$	3Sv
BC-N	160 km	100 km	0 m	$\times$	0 m	0 $cm\ s^{-1}$	0 Sv

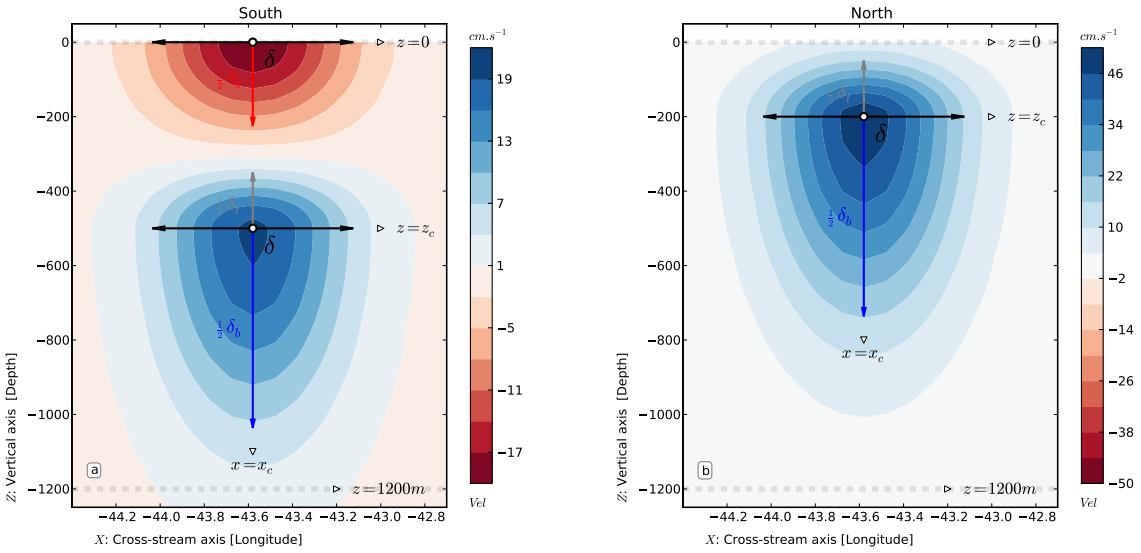

Figure 2.5: Graphical representation of velocity-based stage 1 of the FM system configuration. (a) cross-sectional velocity distribution in the southern edge of the domain with pertinent parameters representation. (b) same, for the northern edge of the domain. For simplicity, a linear NBUC northward surfacing and growth is adopted, as well as a linear southward BC growth.

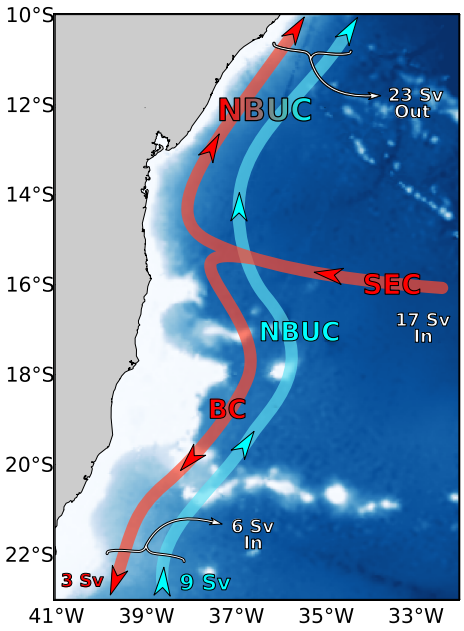

Figure 2.6: Volume transport values imposed in the borders of the EBRA domain via the application of the BC-NBUC-SEC feature models for the control experiment. Note that the sensitivity experiments will be thoroughly detailed in Section 2.3.2.

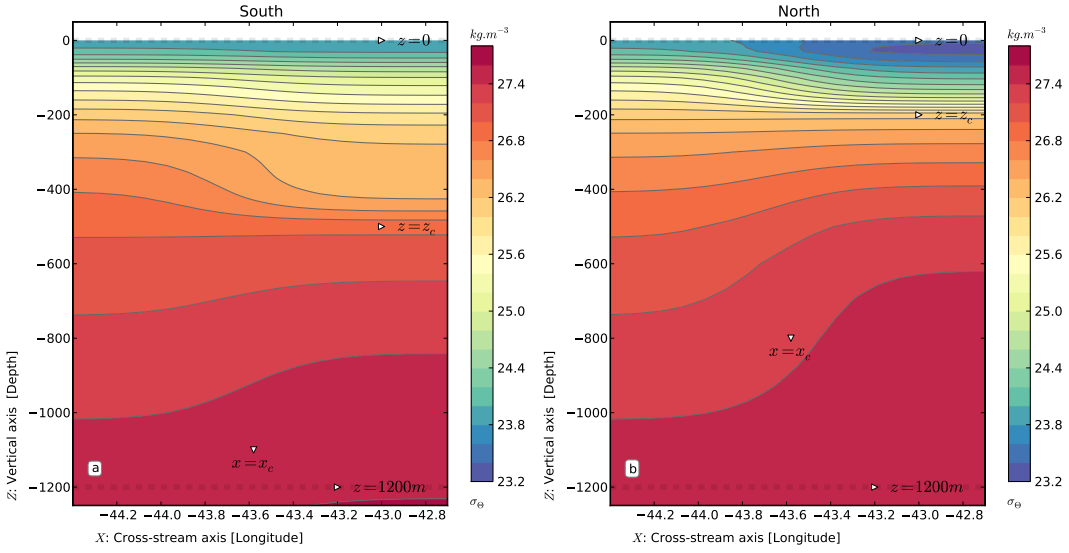

Figure 2.7: Cross-sectional geostrophically balanced σ_θ distributions in the (a) southern and (b) northern edges of the domain.

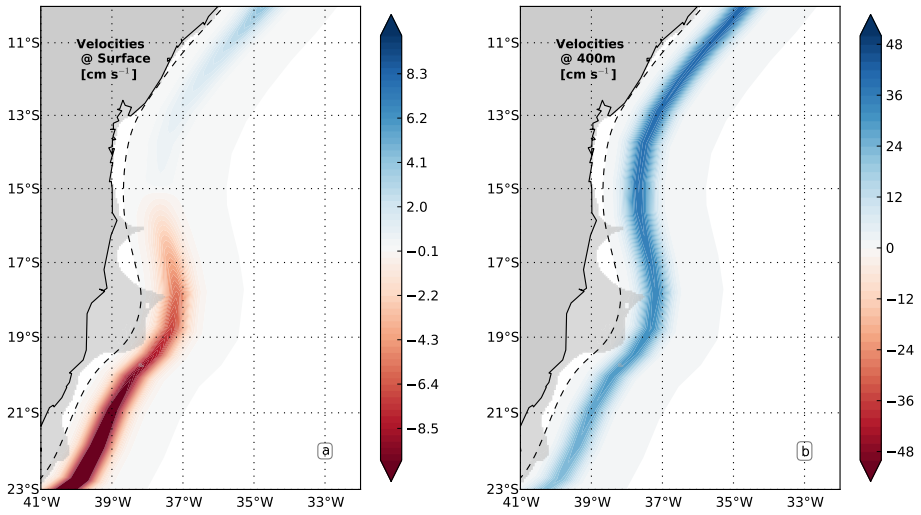

Figure 2.8: Along-shelf velocities horizontal maps for surface (a) and 400 m (b). The gray shade represents depths shallower than 100 m and the dashed line is the smoothed shallow-deep ocean interface that serves as origin for the FM transects. Note the limit between surface southward (BC) and northward (NBUC) flow at 15°S representing the BiSEC signature at the western boundary. Note also the strengthening character of NBUC at 400 m.

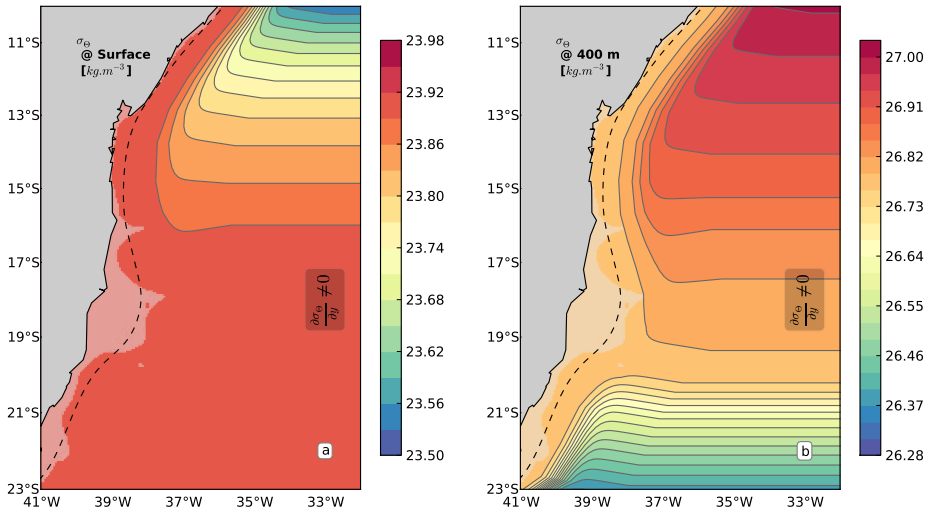

Figure 2.9: Horizontal σ_θ maps for surface (a) and 400 m (b). The gray shade represents depths shallower than 100 m and the dashed line is the smoothed shallow-deep ocean front that serves as origin for the FM transects. Note also the meridional density gradient resulting from the meridionally growing BC-NBUC system.

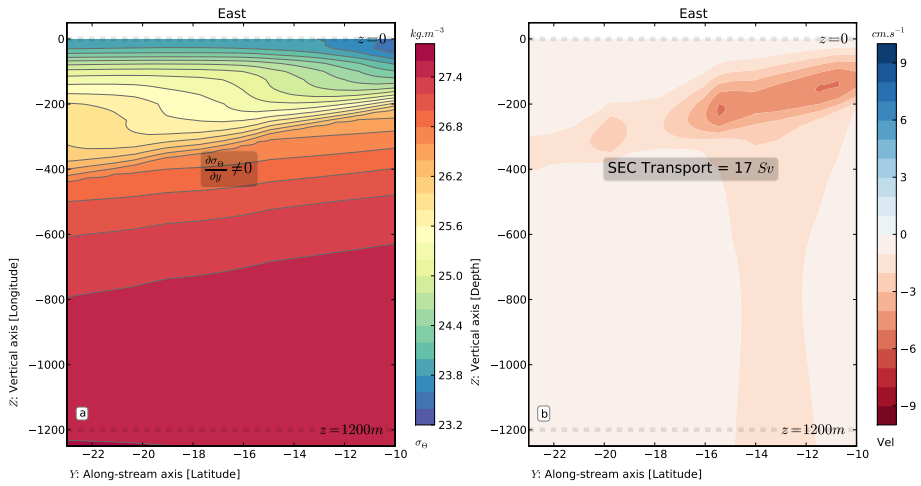

Figure 2.10: Cross-sectional distributions of (a) σ_θ and (b) velocities for the SEC feature model.

The $T - S$ fields, which are actually required for the primitive equation model as initial and boundary conditions, are computed through

$$\rho(x, z) = \bar{\rho}[1 + \bar{\beta}S_0(z) - \bar{\alpha}T(x, z)], \tag{2.7}$$

which is a bi-dimensional linearized equation of state used by *Fernandes* [2007]. Mean haline contraction coefficient is represented by $\bar{\beta}$ (8.0×10^{-4}), $\bar{\alpha}$ is the mean thermal expansion coefficient ($2.2 \times 10^{-4}\ ^\circ C^{-1}$) and S_0 is a mean S profile computed from climatology. Temperature is then computed by re-arranging Eq.2.7 as

$$T(x, z) = \frac{\frac{-\rho}{\bar{\rho}} + 1 + \bar{\beta}S_0(z)}{\bar{\alpha}}. \tag{2.8}$$

And finally salinity is obtained following *Fernandes* [2007] by Eq.2.9,

$$S(x, z) = S_0(z) - 10^{-2}T(x, z). \tag{2.9}$$

In stage 3, it is aimed to include SEC flow to complete the velocity FM system. The density and $T - S$ fields already contains the adequate baroclinic pressure gradient (Figure 2.9). The model domain $T - S$ fields are completed towards the ocean interior by repeating the last values of the FM transects, as shown in Figure 2.9. Since we know

that in our idealized EBRA system the velocities are zero at the bottom, it is straightforward to compute SEC geostrophic velocities from this density field considering 1200 m as a level of no motion. The resulting SEC velocities are shown in Figure 2.10b. The SEC volume transport is equal to the imbalance of 17 Sv generated by the BC-NBUC system (see Table 2.2). This SEC velocity field is them repeated column-wise towards the western boundary of EBRA up to a distance of 100 km of the easternmost FM transect, being damped to zero within this range. This SEC zonal velocity field is then interpolated together with the BC-NBUC system in the model grid. The thermohaline fields are also interpolated to this grid, getting ready to serve as initial conditions to the primitive equation model.

Finally, in stage 4, to complete the prognostic variables required by the numerical model, depth-averaged flow and SSH are computed. In that case, SSH is simply computed through

$$SSH = \frac{\Delta\Phi}{g}, \tag{2.10}$$

where the geopotential anomaly ($\Delta\Phi$) is obtained through S and T using again 1200 m as level of no motion. Figure 2.11 shows the SSH and depth-averaged velocity fields require by the numerical model as initial and open boundary conditions variables.

2.3.2 Model Implementation and Experiments

The primitive equation model chosen for this study is the Regional Ocean Modeling System (ROMS) [*Shchepetkin & McWillians*, 2005]. ROMS has curvilinear horizontal coordinate system and terrain-following in the vertical. The model domain for EBRA has a $1/24^\circ$ resolution with 179 x 271 grid points, which results in a 1000 km x 1440 km area (23°S to 10°S and 41°W to 32°W) as in Figure 2.12. The total number of vertical levels is 20. Topography is configured in different ways for different experiments. For the realistic topography experiment, ETOPO1 is truncated in 1500 m and than interpolated to the grid (2.12a), minimizing pressure gradient errors by restricting the bathymetry gradients under an r-factor of 0.2 [*Haidvogel et al.*, 2000]. For the flat bottom idealized topography, a mean shelf/slope is computed for the region and repeated throughout

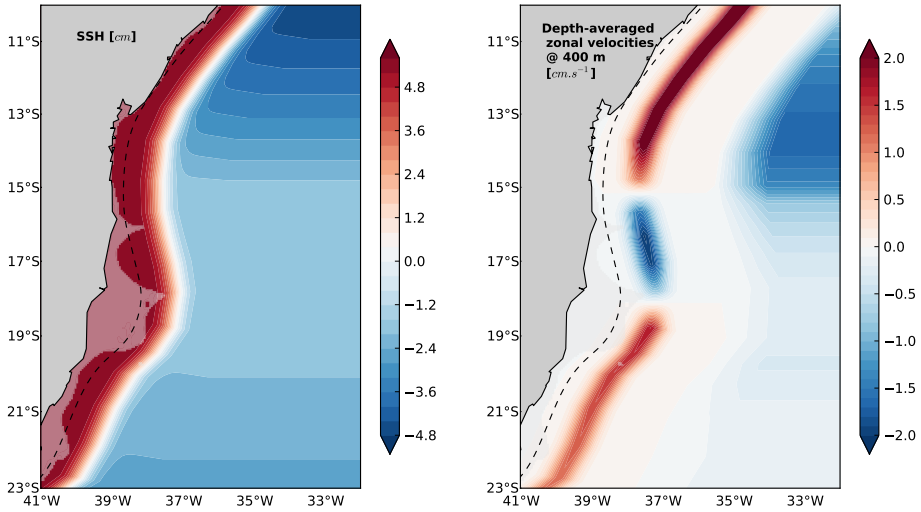

Figure 2.11: Horizontal SSH (a) and depth-averaged velocity (b) maps The gray shade represents depths shallower than 100 m and the dashed line is the smoothed shallow-deep ocean front that serves as origin for the FM transects.

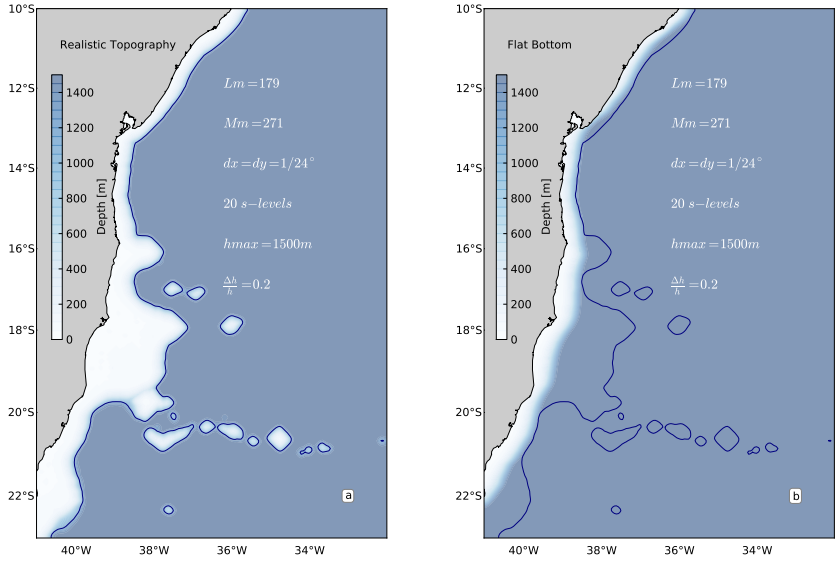

Figure 2.12: Numerical model grid for the two different bathymetric configurations. (a) ETOPO 1′ real topography truncated in 1500 m and (b) flat bottom without banks. Model domain0 setup information is shown. The realistic 1000 m isobath is plotted as blue line in both panels.

the EBRA domain (Figure 2.12b).

Vertical mixing of momentum, T and S is done by the k-profile turbulent closure model by *Large et al.* [1994]. Harmonic horizontal mixing and diffusivity are used both with 5 m^2s^{-1} coefficients in the interior of the domain and a mild sponge layer of six grid points is applied at the open boundaries (N, S, E), linearly increasing the viscosity up to 50 m^2s^{-1}. At the three open boundaries, we follow *Peliz et al.* [2003] approach by keeping the FM fields nearly steady through the use of strong relaxation in a layer of six grid points. Nudging time scales vary from 6 to 1 day from the interior to the boundary. In order to avoid reflections of the flow, additional active/passive conditions were also used at the boundaries [*Marchesiello et al.*, 2001], with strong inflow time scale of 1 day.

In all the experiments, the FM field is interpolated to ROMS grid with its particular bathymetry setup. No other forcing are imposed, so all the dynamics are consequence of one year evolution of the initial field interacting with itself and the topography. A total of three sensitivity experiments were carried out to study the mechanisms proposed as scientific hypothesis of this study. Table 2.3 summarizes those experiments and Figure 2.13 their schematic setup. The results of the different experiments will be described in different sections. For each experiment, a brief description of the model run will proceed the presentation of its results.

Table 2.3: Configuration of the different numerical experiments performed. In the table, *ID* stands for the name of the experiment, *IC* stands for initial conditions and *TOPO* stands for topography.

ID	IC	TOPO
CONTROL	BC, NBUC, SEC	Realistic
S1	BC, NBUC, SEC	Flat bottom, no banks
S2	BC, SEC	Realistic

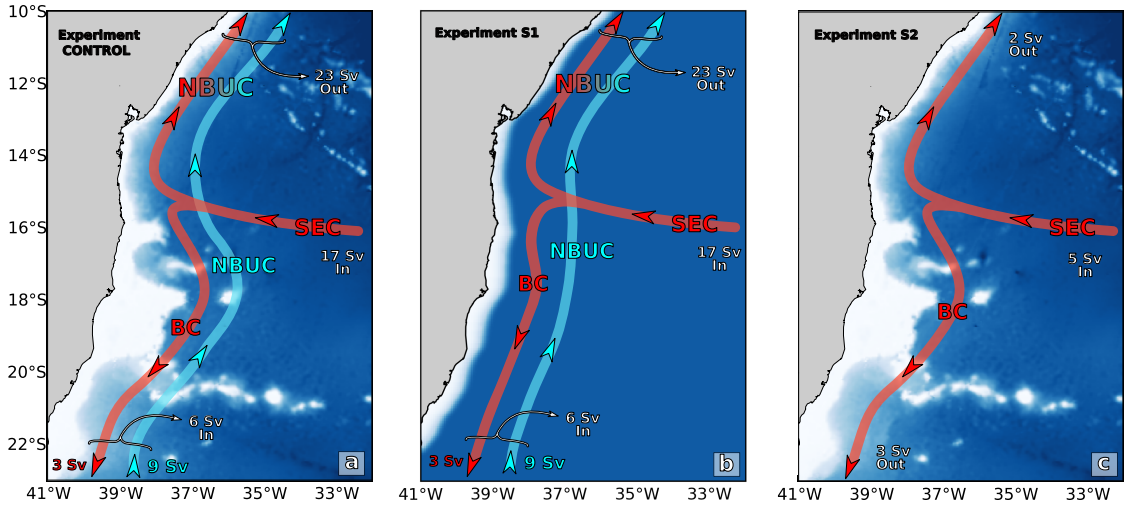

Figure 2.13: Schematic setup of the different numerical experiments performed showing the jets and topography. (a) CONTROL experiment. (b) S1 experiment. (c) S2 experiment.

2.4 Experiments Results

2.4.1 BC/NBUC with Realistic Topography

The CONTROL experiment accounts for the fully designed system described in Section 2.3.1, i.e. the dynamically balanced BC-NBUC-SEC feature models with realistic topography (Figure 2.13a). In the first 10 days, the prescribed feature model system appears to go through a spin-up phase, where the smooth geostrophically balanced jets adjusts to the topography. Figure 2.14 shows the domain-averaged kinetic energy evolution during the year-long simulation as a proxy for dynamical equilibrium during the three runs. The short adjustment phase is an advantage of the FM backward approach [*Calado et al.*, 2008], where geostrophically balanced velocities and termohaline fields in a mass conserving 3D field are both available since the beginning of the time integration.

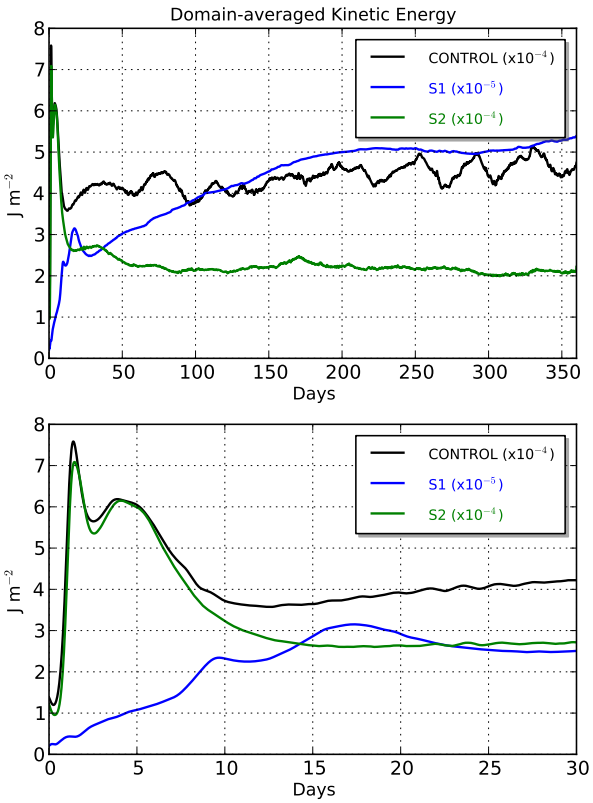

Figure 2.14: Domain-averaged kinetic energy for the CONTROL experiment: (a) the entire simulation period, and (b) a zoom on the first 30 days of simulation.

We selected one representative synoptic sequence of the near-surface flow to exhibit the mesoscale activity developed during the run. The total velocity maps for the first 30 days at 100 m are shown in Figure 2.15 and the vertical sections of meridional velocity are shown for four different latitudes in Figure 2.16. By day 10, we note the regional adjustment of a bifurcation at the tip of RCB, splitting into the two WBCs (BC and NBUC), as intended by the designed FM field. At this time, BC and NBUC are flowing above of the continental margin, smoothly following its bathymetric contours. No significant eddy activity is noted. At day 20, after this initial adjustment stage, the BiSEC appears to shift northward up to 15°S, which is consistent with previous studies [*Stramma & England*, 1999; *Rodrigues et al.*, 2007]. We start to note relevant eddy activities at this point. A large cyclonic eddy possibly associated with the BiSEC and the NBUC is developed at 13.5°S and this feature is very similar to one observed in Feb 2005 (*Soutelino et al.* [2011], Chapter 1, Figure 2.17). At the BC domain, the flow responds to topography and evidence of formation of anticyclone is noted at the luff of RCB and AB (with respect to BC flow) and just off AB. By day 30, two anticyclones are fully developed. Hereafter we will refer to them as Ilhéus Eddy (IE, centered at 15.3°S) and Royal-Charlotte Eddy (RCE, centered at 17°S). Their spatial and velocity scales are remarkably similar to those from *in situ* observations (*Soutelino et al.* [2011], Chapter 1). Figure 2.17 gathers these fields to facilitate comparison. The BiSEC is now located at 14.5°S and the 13.5°S cyclone formed on day 20 slightly propagated northward. In general, the modeled field in day 30 is qualitatively and somewhat quantitatively similar to the Feb 2005 VM-ADCP observations, (Figure 2.17). This indicates that the dynamical agents necessary to reproduce the typical mesoscale activity in the region are present in this control simulation. In other words, the dynamically balanced regional setup and interaction of this WBC system within its components and topography appears to be sufficient to generate the major observed mesoscale features. In this experiment, we are particularly interested in investigating the possible recurrence or stationarity of these anticyclones, which is described next.

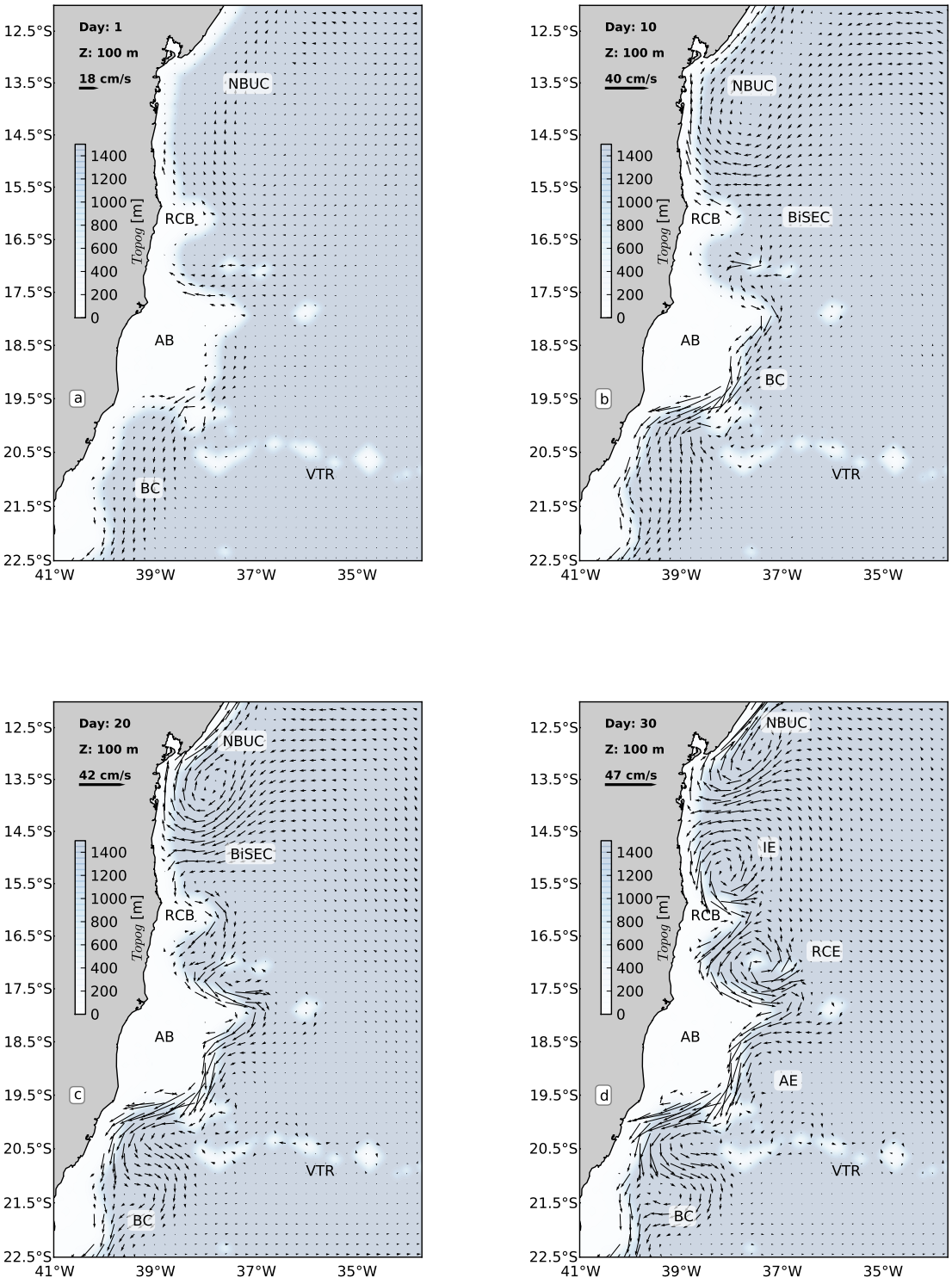

Figure 2.15: Synoptic velocity fields at 100 m for the CONTROL Run. (a) day 1, (b) day 10, (c) day 20 and (d) day 30.

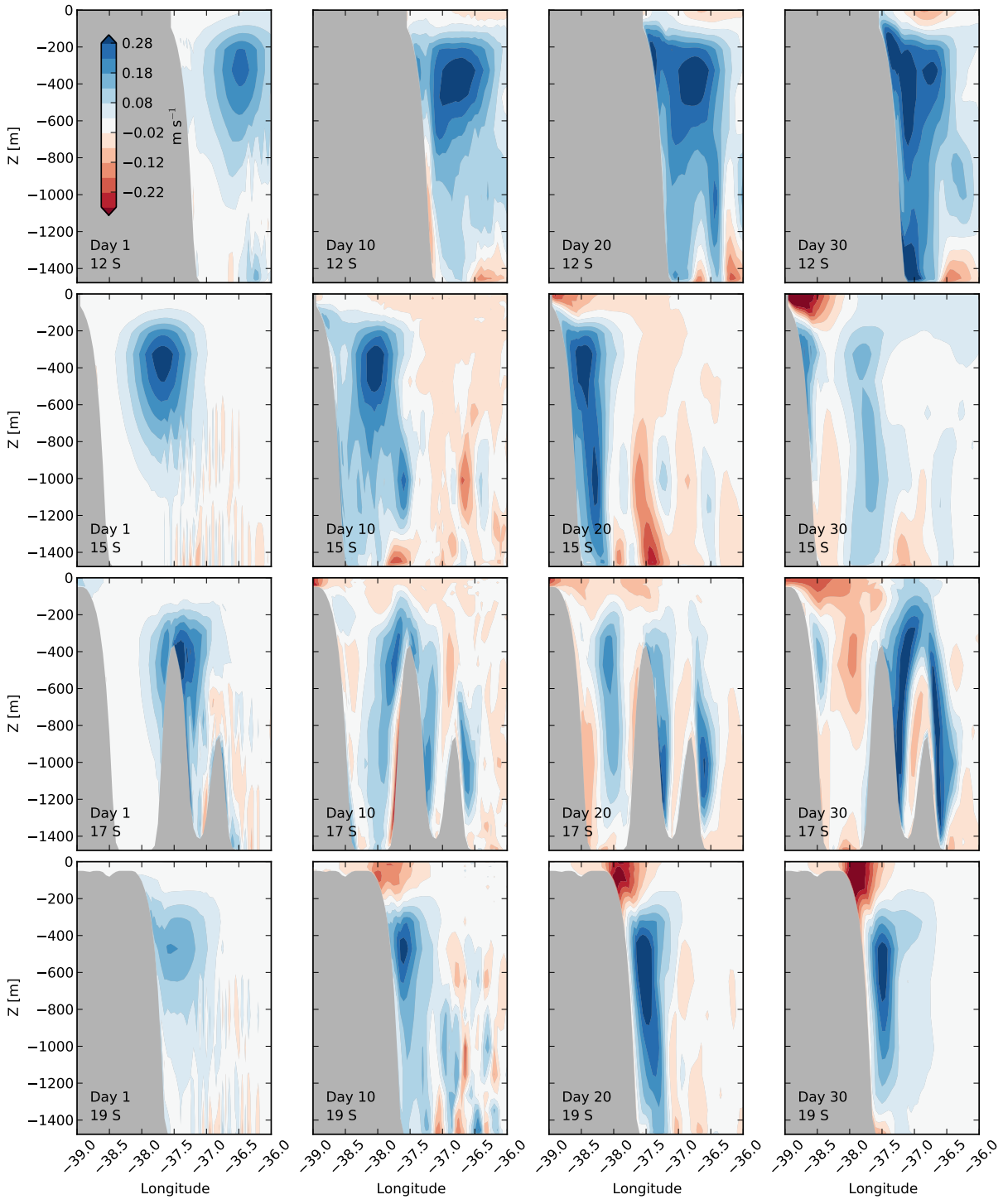

Figure 2.16: Synoptic meridional velocity vertical sections at 19°S, 17°S, 15°S, 12°S (rows) for days 1, 10, 20 and 30 (columns) for CONTROL experiment.

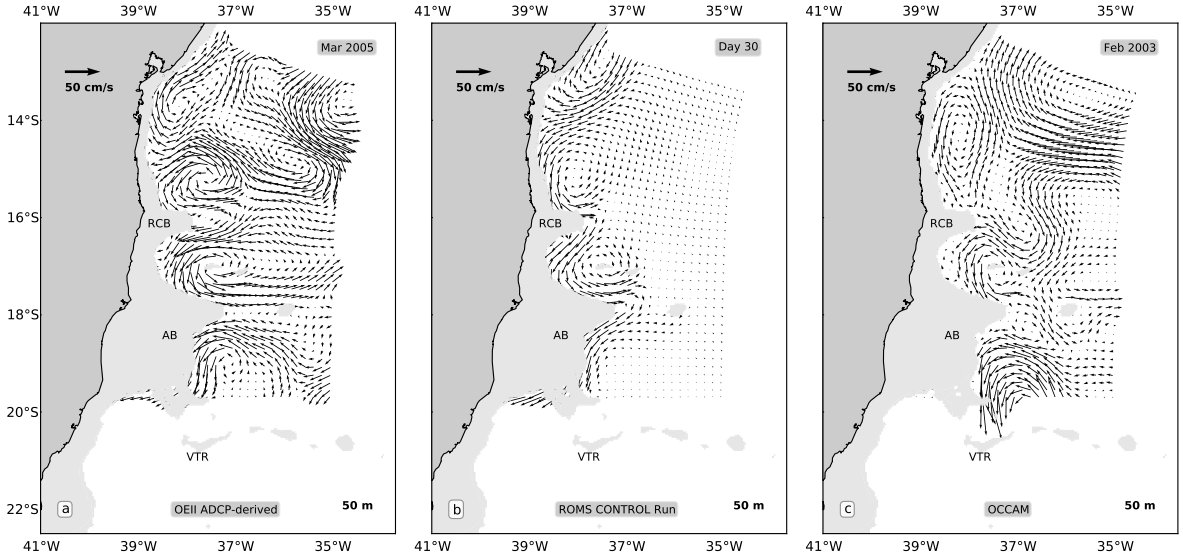

Figure 2.17: Comparison of the velocity fields from *Soutelino et al.* [2011] (Chapter 1) with the one obtained in this work. (a) OEII observed velocities for March 2005. (b) ROMS CONTROL run at day 30. (c) OCCAM February 2003 average velocities. For the sake of comparison, ROMS velocities were interpolated to the same grid adopted to map the observed data sets

The analysis of three-month averages enables us to have a general idea of the velocity fields during most of the run. In Figure 2.19, we show the averages for the periods of 90-120 days, 150-180 days, 210-240 days and 270-300 days. In all the cases, both IE and RCE remain fully developed and steady at the location they were initially originated. A new anticyclone is formed offshore AB (Abrolhos Eddy, AE) and stays steady during the remaining of the run. The steady characteristic of IE, RCE and AE is not repeated by other structures throughout the domain. During the run, we note eddy-flow and eddy-eddy interactions that allows for the formation of other mesoscale features that propagate and either dissipates or grows. One example would be the cyclone associated with the NBUC in the northern portion of the domain (13.5°S). This feature is formed and propagates northward during the run, as in the case of Figure 2.15 and panels c-d of Figure 2.19. Another feature that we highlight is the cyclonic eddy formed in the lee of AB (20°S). This feature is very similar to the VE, cited in Section 2.2, which was studied by *Schmid et al.* [1995], *Campos* [2006], and also recently addressed by *Arruda et al.* [subm]. We note that the VE develops by day 60 (not shown here) and slightly grows as it slowly translates northeastward, appearing to be trapped

by VTR seamounts. This translation pattern roughly agrees with one of the modes suggested by *Schmid et al.* [1995], *Campos* [2006] and *Arruda et al.* [subm].

Continuing with the time-averaged fields analysis, Figure 2.20 shows run-averaged fields. Those were computed from day 30 to the end, to avoid the spinup and initial eddy development phase. The presence of IE, RCE and AE in the near-surface fields (1 and 100 m, panels a and b) is an evidence of stationarity of these features. Note the similarity between the modeled 100 m (Figure 2.20b) field and the OCCAM 2003 averaged field from *Soutelino et al.* [2011]-Figure 1.7a. Evidences of all three anticyclones were also reported on the recent results of *Arruda et al.* [subm] using satellite-derived altimetry and a *Hybrid Coordinate Ocean Model* (HYCOM) implementation outputs (Figure 2.18).

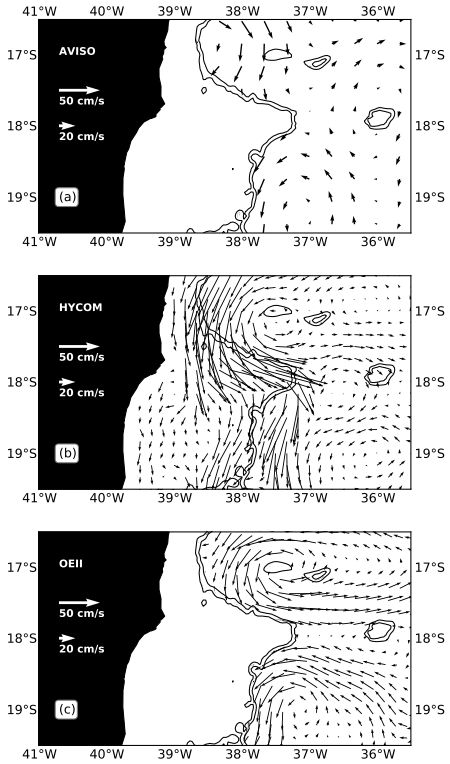

Figure 2.18: Comparison between altimetry (a), HYCOM (b) and *in situ* (c) velocities in March 2005. Adapted from *Arruda et al.* [subm].

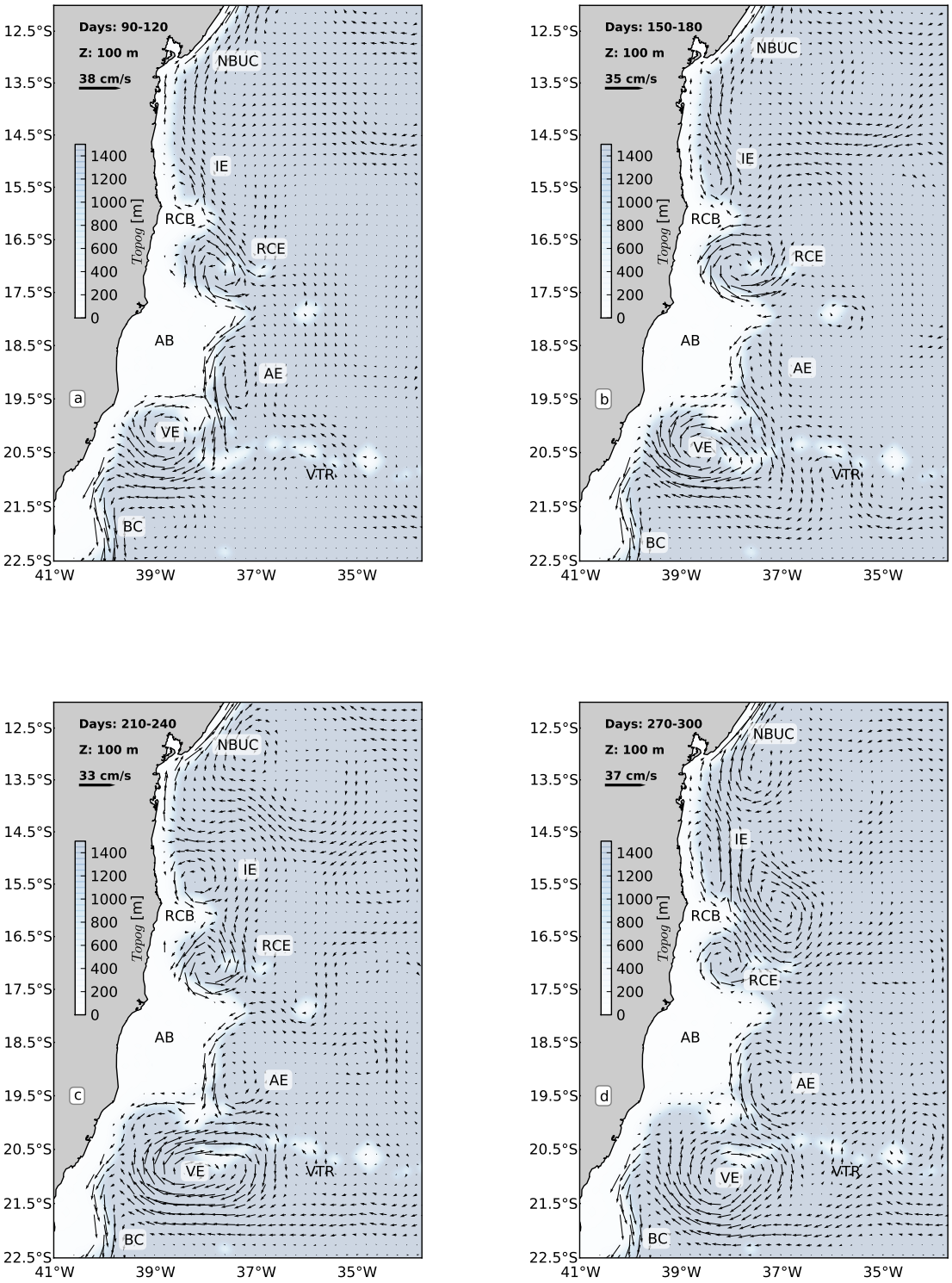

Figure 2.19: Monthly-averaged velocity fields at 100 m for the CONTROL Run. (a) Days 90-120 average, (b) days 150-180 averages, (c) days 210-240 averages, (d) days 270-300 averages.

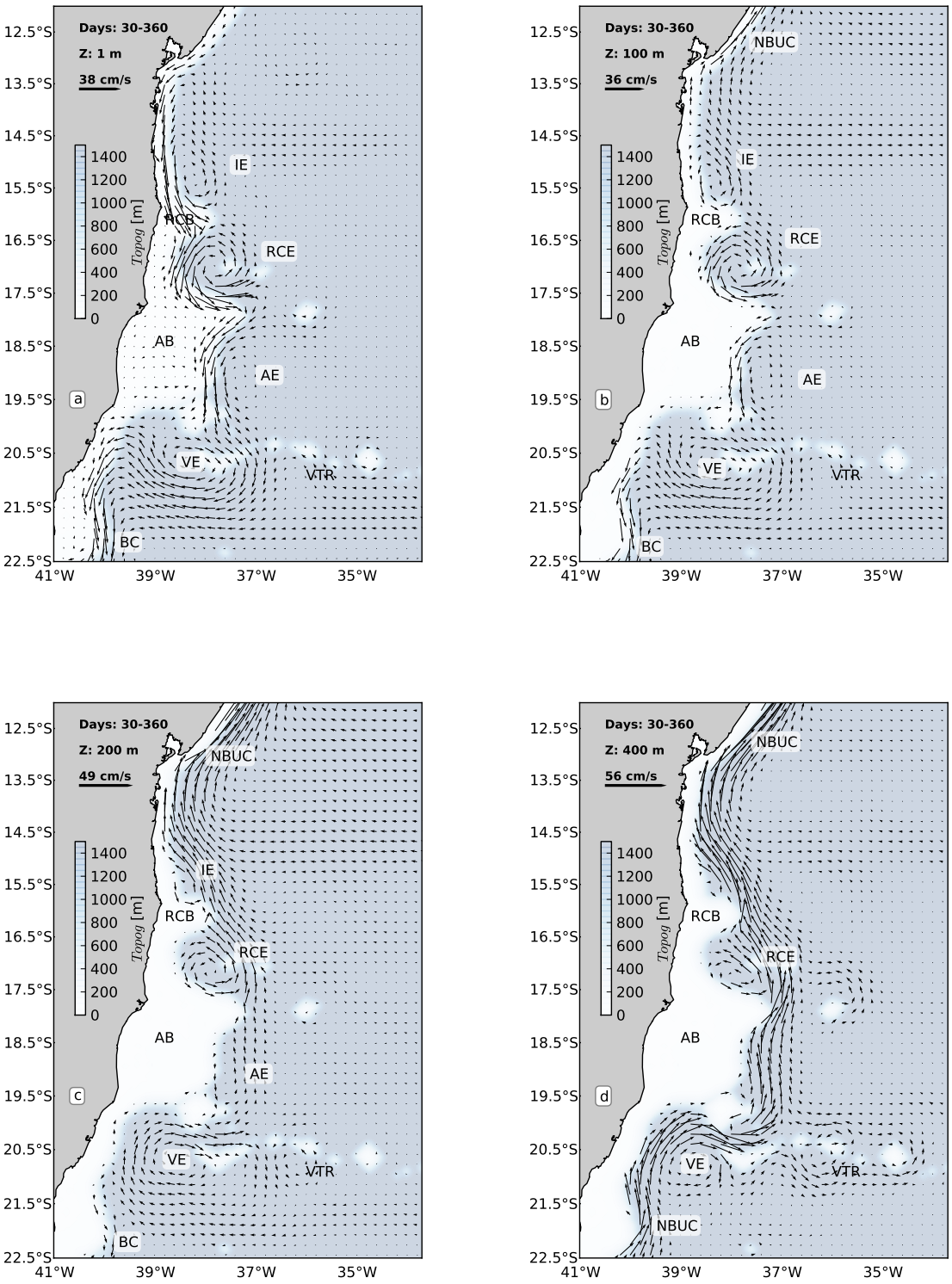

Figure 2.20: Yearly-averaged velocity fields for the CONTROL Run: (a) 1 m, (b) 100 m, (c) 200 m, (d) 400 m.

Looking at deeper levels we note that the anticyclones are mostly inexistent at 400 m (Figure 2.20d). The IE and AE signatures are poor at 200 m (Figure 2.20c) and RCE is the deepest one, with signal reaching 400 m (Figure 2.20d).

The analysis of synoptic and time-averaged fields of the main experiment supports two statements. The first one is that BC-NBUC shear and realistic topography are sufficient mechanisms to the development of realistic mesoscale activity previously observed in the region. Through the analysis of the further and simpler sensitivity experiments (Sections 2.4.2 and 2.4.3) we intend to find out if this sort of activity can or cannot be developed when removing one of these mechanisms. The second one is that the EBRA region under this forcing exhibited the formation of three steady mesoscale anticyclones that lasted the entire run.

2.4.2 BC/NBUC with Flat Bottom

This experiment is designed to study the impact of the BC-NBUC shear on generating eddies without the influence of topography, i.e., the presence of the banks (the RCB and the AB). The flat-bottom topography is built by implementing a *bank-free* continental margin extracted from the northern part of EBRA. This topographic profile does not vary in the along-coast direction, e.g. no banks, promontories or seamounts (Figure 2.12b). The FM formulation is essentially the same, except from the BC-NBUC along-shelf trajectory, which is smoother (Figure 2.13b).

During this run, very occasional eddy activity is noted, far less than what was noted in CONTROL run. In order to illustrate the modeled scenario, Figure 2.22 shows the synoptic meridional velocity vertical distributions up to day 90 and Figure 2.21 shows the run-averaged velocity fields in BC and NBUC typical depth levels. Figure 2.21a shows that in the BC domain, the BiSEC occurs at higher latitude (19°S) when compared to the CONTROL run. From that latitude, NBUC seems well organized, stable and is intensified towards the northern part of EBRA. BC flows southward from BiSEC latitude with only one evidence of eddy activity at 22°S. At 400 m (Figure 2.21b, NBUC flows continuously throughout the domain.

The results of this experiment emphasizes the importance of realistic topography and indicate that the shear between the BC and the NBUC cannot, by itself, generate

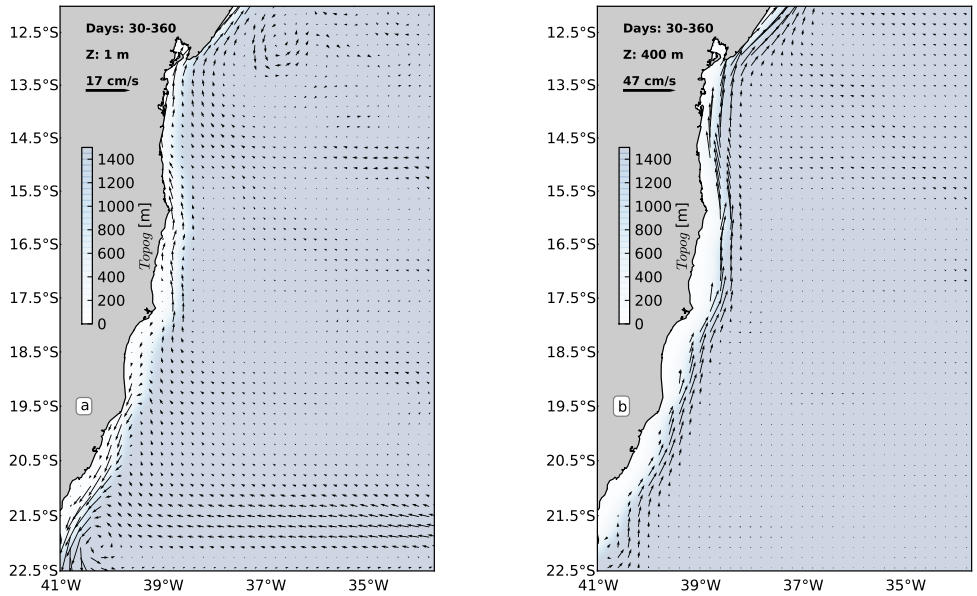

Figure 2.21: Yearly-averaged velocity fields at (a) 50 m and (b) 400 m for the S1 experiment.

and sustain all realistic eddies along the BC formation region, at least with this feature-modeled configuration.

2.4.3 BC with Realistic Topography

A second sensitivity experiment (S2) is designed to isolate the topography-related instabilities as a trigger to the observed BC mesoscale activity. By keeping the realistic topography and removing the NBUC flow, we obtain evidences of the importance of BC-topography interaction to the overall pattern. To create the initial fields, we remove the NBUC-FM and adapt the BC-FM to keep the surface northward flow at the north of EBRA active in the system. In order to do that, we simply allow BC core velocities to intensify from 0 m s^{-1} by changing the $\delta_b/2$ and v_c parameters in Table 2.2 to 150 m and 10 cm s^{-1} respectively. This value for v_c matches from the velocity of NBUC at surface in the CONTROL experiment initial field. Without the NBUC, the SEC resulting volume transport is smaller in this case, to maintain mass balance. Figure 2.13c illustrates this setup. The spin-up phase for S2 took about 20 days, as shown in Figure 2.14. The kinetic energy in S2 run is nearly one order of magnitude smaller than in CONTROL run, which is expected due to the absence of the undercurrent.

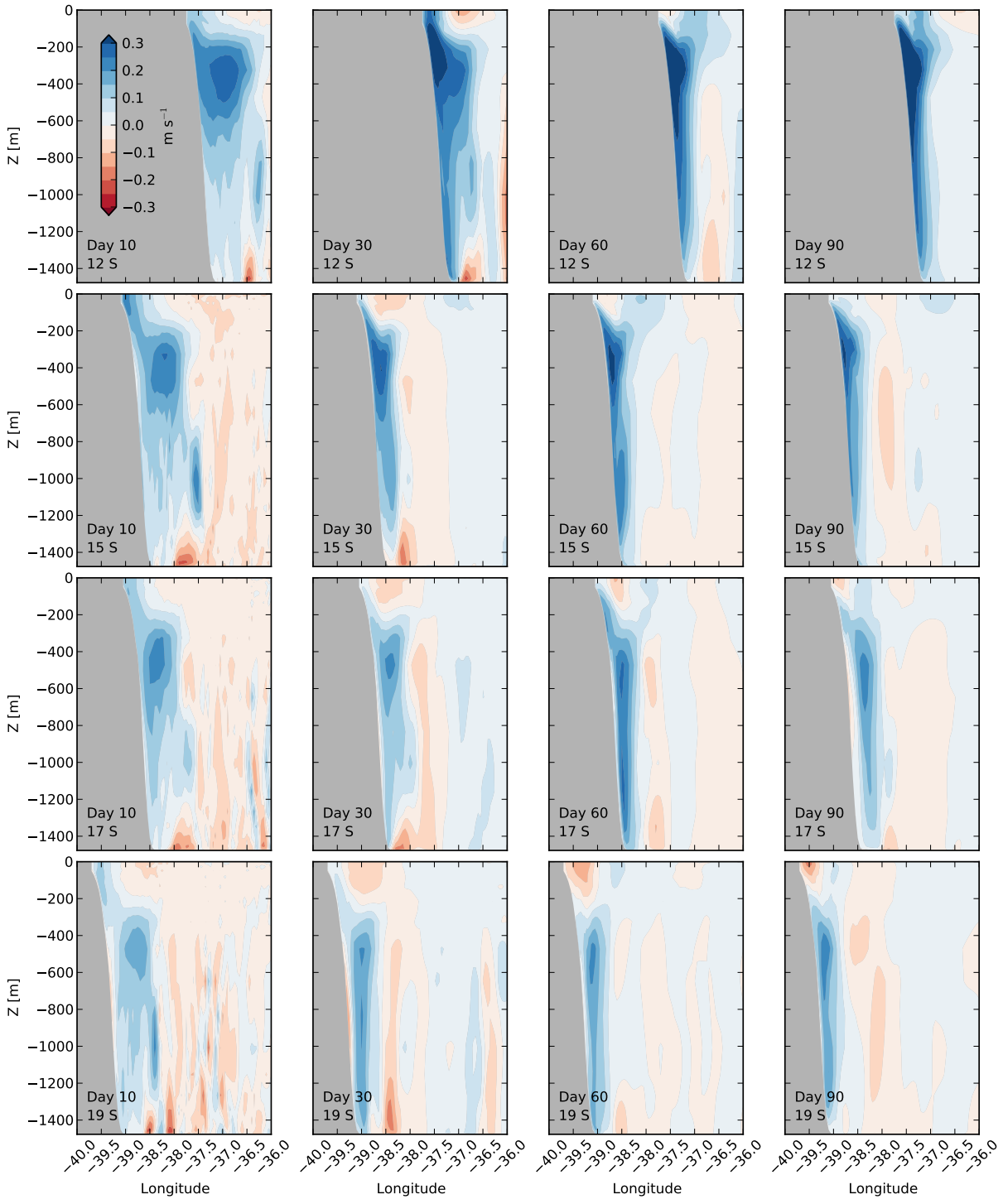

Figure 2.22: Synoptic meridional velocity vertical sections at 19°S, 17°S, 15°S, 12°S (rows) for days 10, 30, 60 and 90 (columns) for S1 experiment.

From day 1 to day 10, the flow adjusts to topography (Figures 2.23 and 2.24). At day 30, still no mesoscale activity is observed. The first evidences of eddy activity appears only at day 60, where two topography-related cyclones develops at the lee of RCB and AB. Other cyclonic eddies are formed offshore and are probably associated with the seamounts and the VTR. By day 90, these cyclones are better defined and stronger, and an additional one (VE) is formed, but no propagation or growth is noted. The late eddy development compared to the CONTROL run is an indication that the absence of NBUC results in a more stable initial field.

The time-averaged fields (Figure 2.25) for S2 show similar steady and slow propagating characteristics noted in the mesoscale features of the CONTROL run. In S2, the cyclonic eddies formed in the lee of the promontories appear to be steady and non-growing features, probably indicating that the vorticity induced by BC-topography interaction is in balance with vorticity dissipation for EBRA under these conditions. Even VE, which was a growing and eastward slow propagating eddy in CONTROL run, seems to be steady in S2.

According to the results of S2 experiment, the topography still provides sufficient conditions to eddy development at EBRA, but with different types of mesoscale features being formed. Particularly, we note that the BC interaction with topography (S2) gives rise to cyclonic eddies, and BC-NBUC-topography interaction (CONTROL), to anticyclonic eddies.

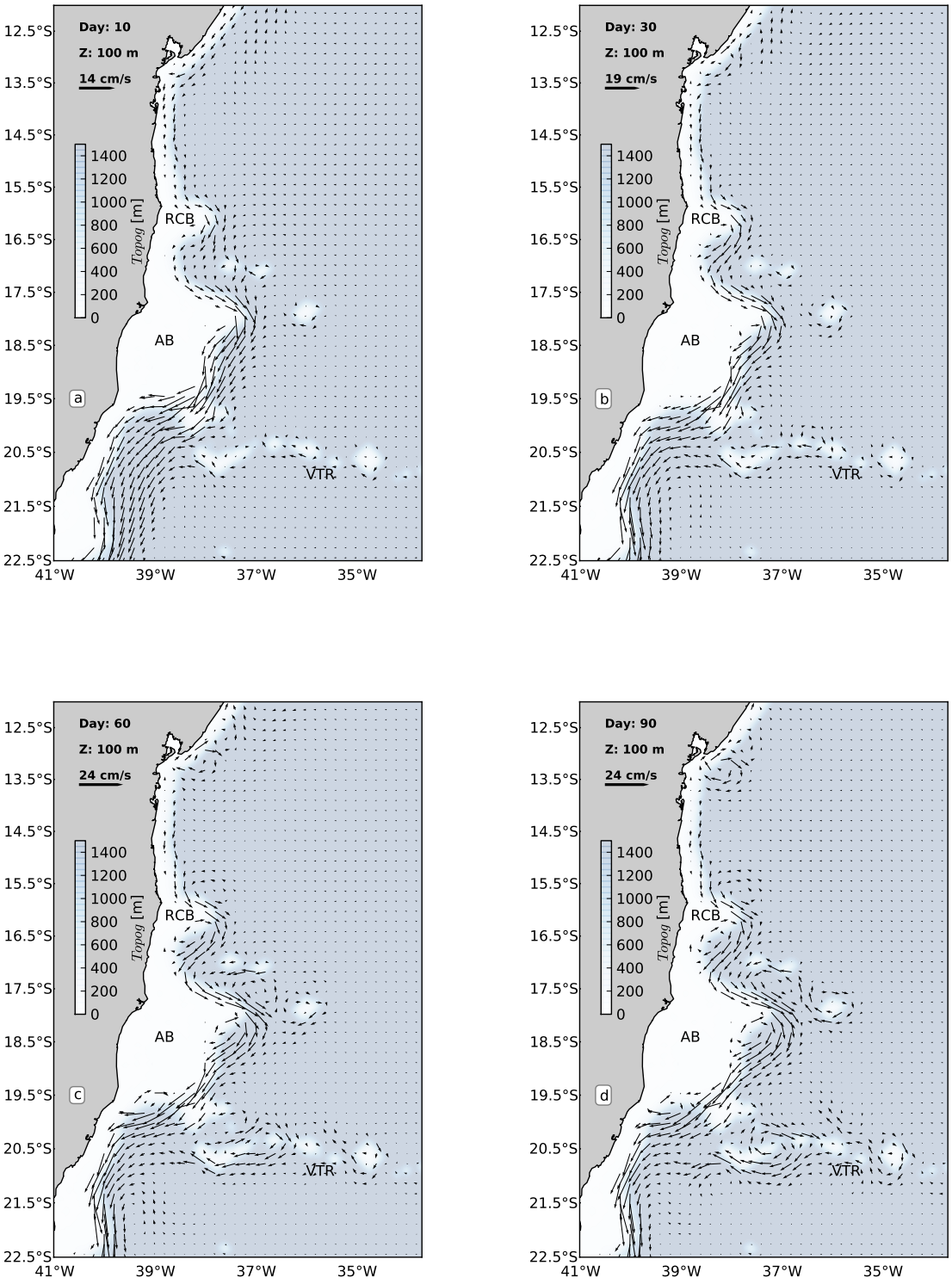

Figure 2.23: Synoptic velocity fields at 100 m for the S2 run. (a) day 1, (b) day 30, (c) day 60 and (d) day 90.

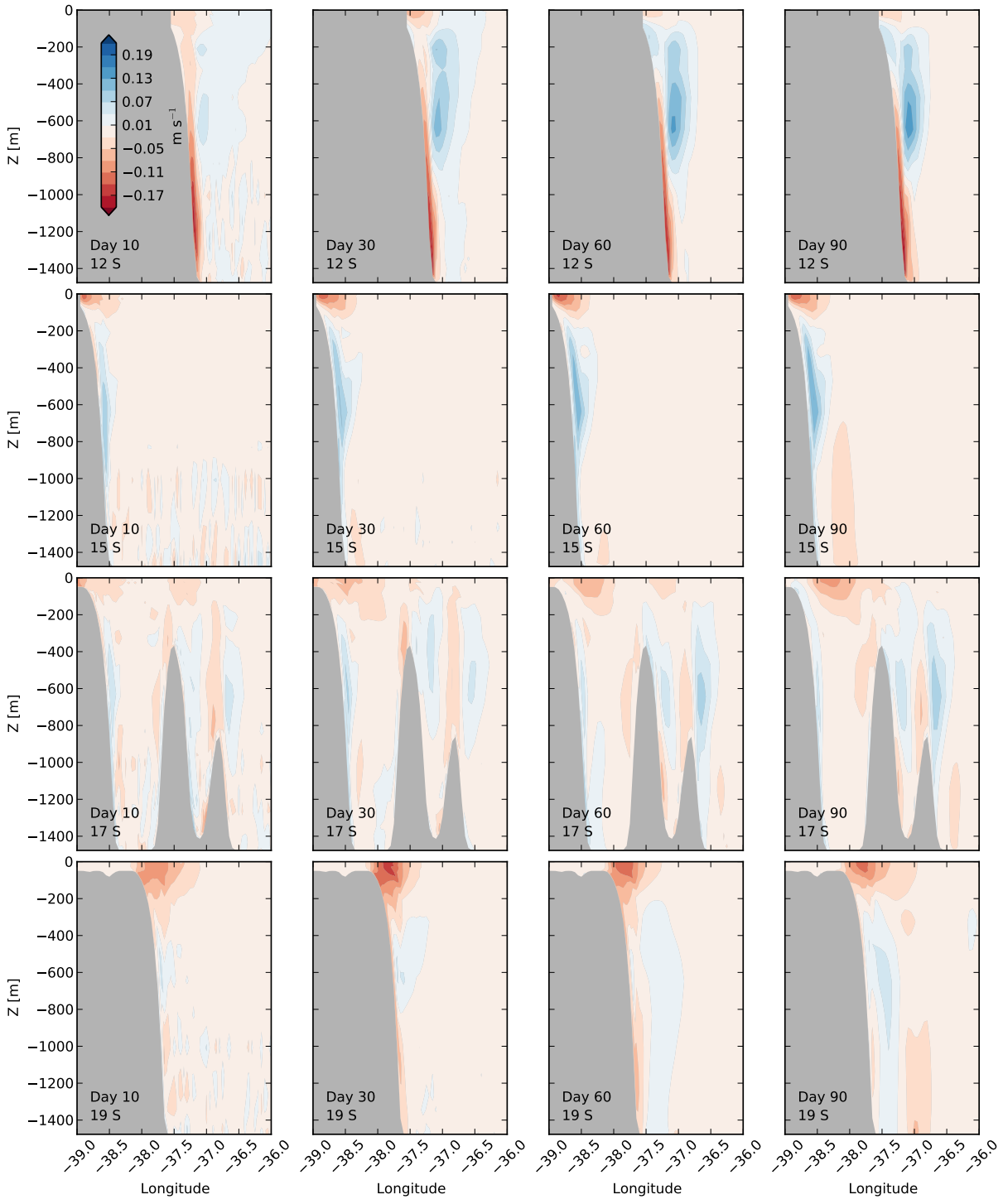

Figure 2.24: Synoptic meridional velocity vertical sections at 19°S, 17°S, 15°S, 12°S (rows) for days 10, 30, 60 and 90 (columns) for S2 experiment.

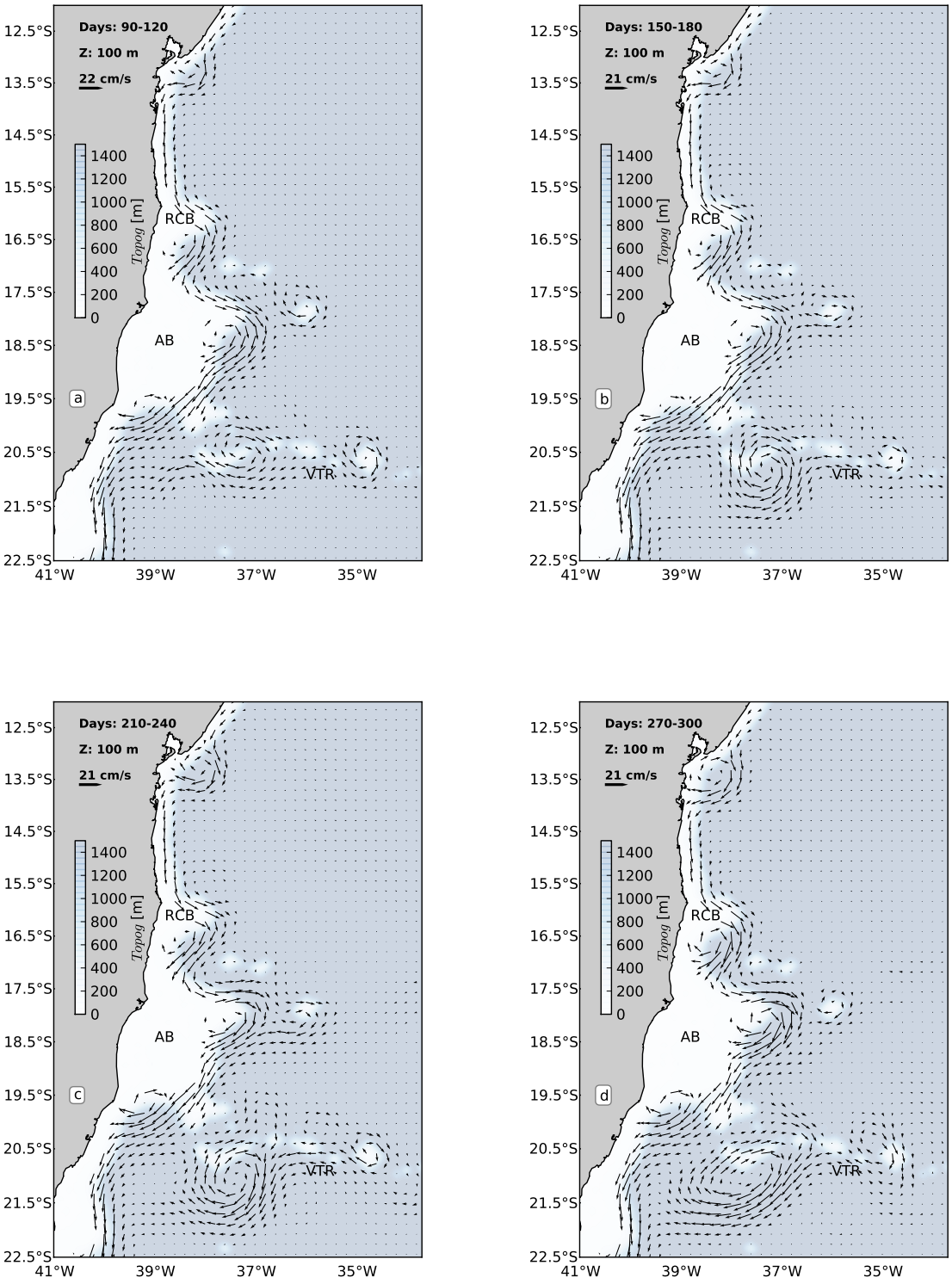

Figure 2.25: Monthly-averaged velocity fields at 50 m for the S2 Run. (a) Days 90-120 average, (b) days 150-180 averages, (c) days 210-240 averages, (d) days 270-300 averages.

2.5 Dynamics of the Eddy Formation

After analysing the three process study experiments described in Sections 2.4.1 - 2.4.3 one can speculate that the existence of the undercurrent (NBUC) is fundamental in the synoptic setup for the reproduction of the realistic mesoscale features. Experiment S2 indicates that the BC flow alone has a preference to evolve to relatively small cyclonic eddies. It is clear that the realistic anticyclones are only formed on the surface when the NBUC flow is present. In this Section, the dynamics of the system will be explored in a quasi-geostrophic (QG) framework, in order to seek a physical explanation for how the NBUC flow is affecting the formation of the surface features. All the model results that are analyzed from now on are related to the CONTROL experiment.

According to *Magaldi et al.* [2008], leeward eddies have been largely observed behind topographic features such as prominent headlands and capes. Eddy generation is connected to the phenomenon of current separation occurring in presence of obstacles. The cyclones formed at the surface in S2 experiment are arguably result of this type of dynamics, where relative vorticity generation combines with the jet inertia as it moves away from the promontories. When an organized jet moves past a promontory, its inertia forces it to separate from the dynamical boundary (i.e., the continental slope). Therefore, at the lee of a promontory, there is a strong velocity gradient between the jet and the steal water left close to the boundary. This velocity gradient characterizes the generation of relative vorticity that forces a re-attachment of the jet to the boundary. Depending on the jet strength and the promontory shape, this mechanism would result in an eddy, which we believe to be the case of our study area.

The above mentioned mechanism may not occur in all types of scenarios. *Magaldi et al.* [2008] did a numerical study to investigate the roles of stratification and topography in generation of eddy structures at the lee of capes. They designed a fully idealized experiment where a steady jet impinges on an obstacle in a rotating and linearly stratified environment. They kept the small Rossby number constant and did sensitivity runs varying the Burger Number,

$$Bu = \frac{R_d}{D}, \tag{2.11}$$

which measures the ratio between baroclinic Deformation Radius (R_d) and the length scale of the obstacle (D). Their results have shown that for $0.1 < Bu < 1$, i.e. $D > R_d$, the jet flows around the obstacle and for $Bu > 1$, i.e. $D < R_d$, eddies emerge in the lee of the obstacle. We computed Bu for both jets offshore AbB, which has the largest radius of curvature, using the expression

$$R_d = \frac{\sqrt{\frac{\Delta\rho}{\rho_0} g H_i}}{|f_0|}, \tag{2.12}$$

to compute R_d. In Eq. 2.12, $\Delta\rho$ is the density step between the two jets, ρ_0 = 1025 kg m^{-3} is a reference density and H_i is the thickness of each jet. We found Bu = 16.61 for BC and Bu = 5.27 for NBUC, which supports the formation of leeward eddies in both cases. That would support the cyclone formation occurring in S2 experiment, for example. Also, one would expect that a northward flow like NBUC alone would generate leeward anticyclones when flowing through the promontories in opposite direction.

In order to provide a dynamical explanation to the formation of surface anticyclones in the CONTROL experiment, where BC and NBUC are together in the initial field, the QG approximation is used. We aim to investigate the model outputs in terms of linear theory for baroclinic geophysical instability, a phenomena that is typical in this type of configuration, where there is a substantial vertical shear in the total flow. Essentially, we will look for energy fluxes between mean and eddy flow.

Before discussing the baroclinic instability aspects, we must first test our case for the validity of the QG approximation. The QG approximation essentially requires that the ageostrophic component of the velocity field is much smaller than the geostrophic one. That translates in a very small Rossby Number. To test this we evaluate the mean Rossby Number for each of the jets during the CONTROL run, following the steps of *Francisco et al.* [2011]. Following these authors we've chosen to compute the Rossby number in the form of the ratio between relative and planetary vorticity,

$$Ro = \frac{|\zeta|}{|f_0|} << 1, \tag{2.13}$$

where f_0 is the Coriolis parameter and ζ is the relative vorticity, defined as

$$\zeta = \frac{\partial v}{\partial x} - \frac{\partial u}{\partial y}, \tag{2.14}$$

where u and v are the velocity components of the flow. To compute Ro, we used the long-term time average flow from the model. Figure 2.26 show the average flow in a zoom at the area where the main eddies were formed (IE, RCE, AbE). Both BC and NBUC levels are shown, as well as a vertical section at 19°S illustrating the system's vertical structure. Note the strong vertical shear of the adjusted time-averaged system. It interesting to compare the vertical structure obtained here to the one initially prescribed by the feature model, shown in Figure 2.5. It shows the successful vertical adjustment of the FMs to the local topography, as well as the ability of the model configuration to maintain the jets alive in the simulation , by successful prescription of open boundary conditions. It is also interesting to note the that the two-layer nature of the system was unquestionably preserved during the model run, with the NBUC being substantially stronger than the BC, as known by previous research. All this encourages us to make the analysis proposed in the following paragraphs.

Figure 2.27 illustrates the Ro horizontal distribution for both jets. For the BC layer, the average value is Ro = 0.008 and the maximum value is Ro = 0.06. For the NBUC level, an average of Ro = 0.01 and maximum of Ro = 0.05 were found. Therefore, the values of Ro are much smaller than 1, which leads us to admit the validity of the QG approximation for this study.

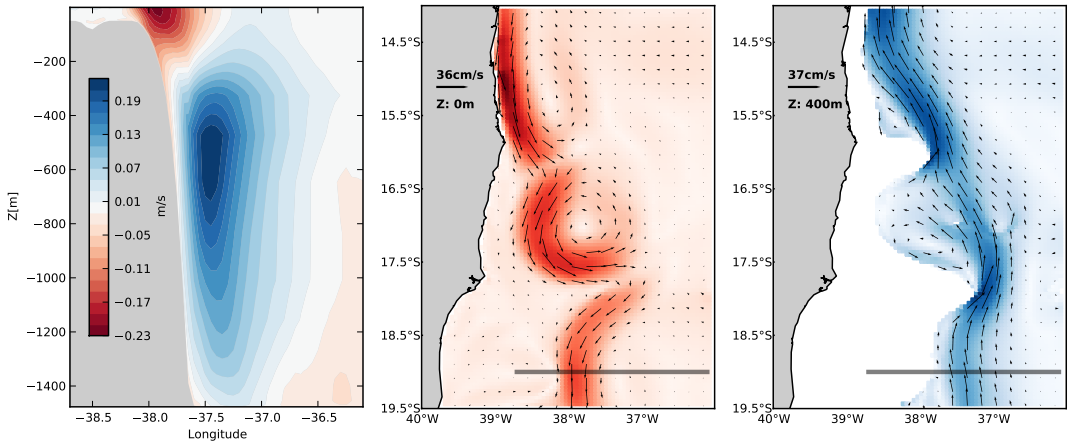

Figure 2.26: CONTROL run-averaged velocity fields. Left: a vertical section at 19°S showing the vertical structure of the BC and NBUC jets. Center: surface run-averaged velocity field. Right: run-averaged velocity field at 400 m

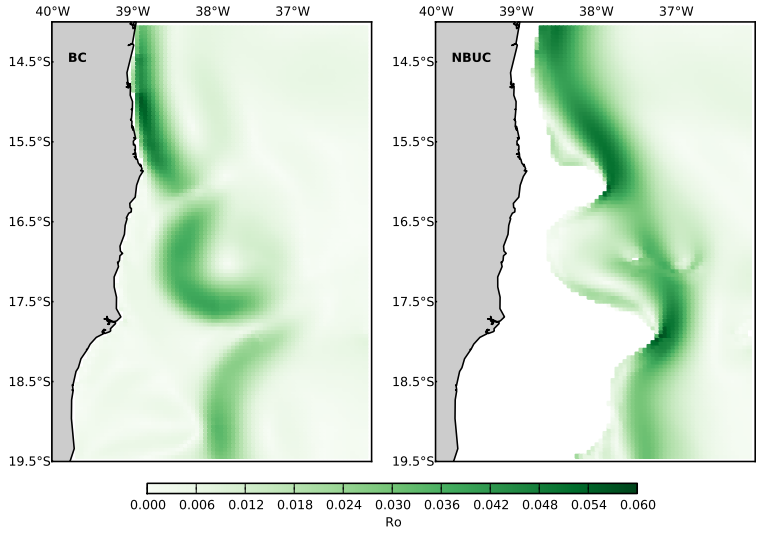

Figure 2.27: Rossby Number (Ro) computation for the BC (left) and NBUC (right) vertical domains. The BC domain is considered surface and the NBUC domain is at 400 m.

Although the interaction with jets and topography discussed in the beginning of this section may explain the origin of meanders in each level separately. However eddy formation and growth may be discussed in terms of baroclinc instability processes, capable of transferring available potential energy from the mean flow to the eddy field.

The structure of the mean modeled flow field is inevitably affected by the existence of perturbations. The perturbations give rise to temperature fluxes and momentum fluctuations through non-linear processes, which results in temporal averages different from zero. Therefore, as defined by *Pedlosky* [1987], the instability phenomena consists in a preferable potential energy transfer from the flow that is free from perturbations to the flow affected by perturbations.

The first step is to investigate whether the idealized BC-NBUC system satisfies the necessary conditions for instability. We use the initial field here, instead of the run average, to test if the designed system itself would be prone to instabilities, since the first eddies appear after the first 30 days of simulation. According to *Pedlosky* [1987] and *Silveira et al.* [2008], in summary, if the vertical profile of cross-jet mean potential vorticity gradient ($\partial\bar{q}/\partial s$) changes sign along depth, all the necessary conditions are satisfied. Figure 2.28 shows the characteristics of the feature-modeled BC-NBUC system that are relevant to baroclinic instability.

It is noted a potential vorticity sign change in the 400 m depth, satisfying the conditions for geophysical instability occurrence. This is a necessary condition, but it does not automatically guarantees the occurrence of instability. In order to verify if there is a baroclinic instability process occurring in the BC domain, we perform energy conversion calculations with the method used by *Cronin & Watts* [1996], and already applied by *Francisco et al.* [2011] and *Mano et al.* [2009] to different regions of the Brazilian coast. The method consists in decomposing the three-dimensional ROMS flow into a high order geostrophic component and a small ageostrophic component. In order to compute the eddy energetics, we must split the instantaneous fields into mean and eddy fields. This is done by defining the mean field as the long term model run average and the eddy field as the deviations from it.

According to *Cronin & Watts* [1996], the baroclinic energy conversion, which is relevant to baroclinic instability, is defined as

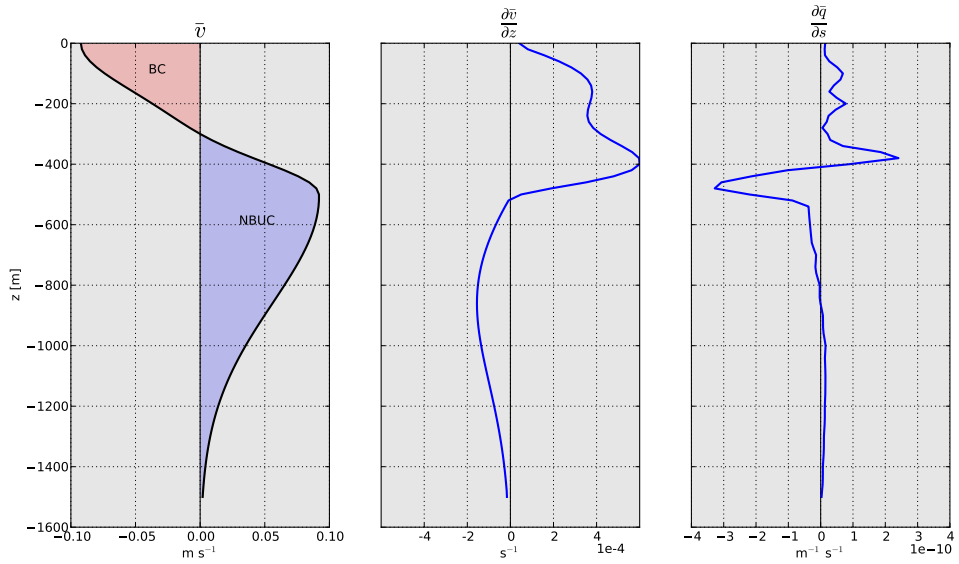

Figure 2.28: Left: mean profile of along-shore velocities for the BC-NBUC feature-modeled system. Center: mean vertical shear of the system. Right: cross-jet mean potential vorticity gradient.

$$EC = \frac{g\alpha}{\theta_z}\left(\overline{u'T'}\frac{\partial \bar{T}}{\partial x} + \overline{v'T'}\frac{\partial \bar{T}}{\partial y}\right), \tag{2.15}$$

where α is the salt contraction coefficient and θ_z a mean vertical temperature profile. The overbars denote time-average and the quotes denote the deviations or perturbations. This expression can be evaluated at any given vertical level of the system. Positive values of EC indicates energy conversion from the mean flow to the perturbations and negative values have no physical meaning, according to *Pedlosky* [1987].

In order to track the energy pathways, we will follow *Mano et al.* [2009] approach. These authors studied a similar problem of eddy formation in the southeast Brazil (23°S). In that area, a similar current-undercurrent (BC-IWBC) interaction occurs. They found out through the analysis of energy conversion during a cyclonic eddy formation event in a numerical experiment, that the following cycle occurs. First there was a well defined flowing BC with a baroclinically unstable profile due to its vertical shear with IWBC flowing in the opposite direction. EC from the mean flow to a perturbation occurs at intermediate (IWBC) depth. The IWBC destabilizes and meanders, followed by the formation and growth of an eddy. EC progressively transfers to shallower depths and the eddy signal propagates upward. In other words, their results indicates that the

eddy first appear in intermediate depths and then in the surface, draining energy from the BC.

One would speculate that this could be the case of the present study. As we show in Figure 2.29e, the first evidence of anticyclone formation (RCE and IE) during the run is noted at 400 m depth, where the NBUC flow is dominant. However, we only note the anticyclone on the surface field (Figure 2.29c) 10 days later. This is quite similar to *Mano et al.* [2009] findings, hence we believe that a similar process is occurring, e.g the surface mesoscale features are being steered by the pycnoclinic flow (NBUC).

In order to verify if this is occurring in our case, we track the behavior of EC in the first 30 days of simulation for the levels of 0 m and 400 m, representing BC and NBUC domains, respectively. We consider the horizontally-averaged EC values, in the area encompassed by Figure 2.29 maps. This region contains both IE and RCE, which are the most developed eddies during the numerical experiment. We followed *Mano et al.* [2009] steps in considering that the horizontal average of EC in a limited area that contains important eddy activity is a good representation of the bulk of baroclinic energy conversion for the system. The first 30 days are chosen because it is when the system move from an idealized, rectilineous, perturbations-free flow to a mature eddy development state. It is an interesting and fairly controlled time period to track the potential energy pathways.

Figure 2.30 shows the result of this analysis. The analysis of Figure 2.30 is done in combination with Figure 2.29. Up to day 10 (spin-up phase) no eddies are observed (Figure 2.29a,d) and the EC values are negative in both levels(Figure 2.30). The EC positive values starts to appear at the NBUC level before day 15. From day 15 to day 20 there is an increase in EC values for NBUC and they reach a maximum value by day 20, while the BC EC values remains negative. This is consistent with panels b and e of Figure 2.29, where there are still no sings of eddies in the BC domain, but there is already a mature RCE and a developing IE at 400 m, which means that there was energy transfer from the mean flow to the perturbations, due to baroclinic instability. NBUC EC values decrease from day 20 to day 25, but are still positive, which probably explains more growth to the RCE and final development of IE, culminating in day 30 (Figure 2.29f). It is interesting to note that positive EC values for BC started occurring

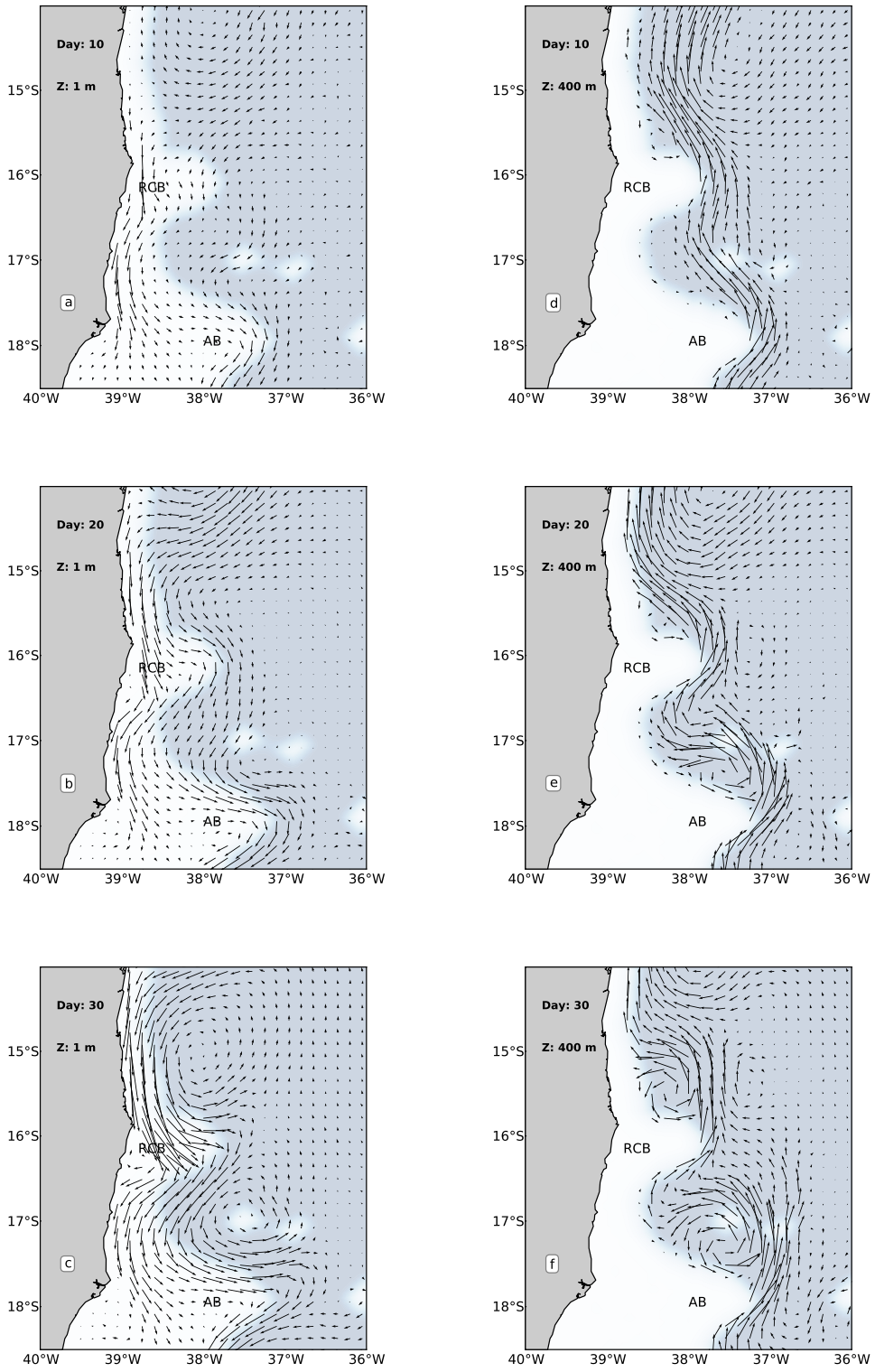

Figure 2.29: Synoptic velocity fields for the CONTROL Run in days 10, 20 and 30, zooming in the region where IE and RCE are developed. (a-c) at surface and (d-f) at 400 m. Note the formation of the eddies occurs at 400 m 10 days before it occurs at surface.

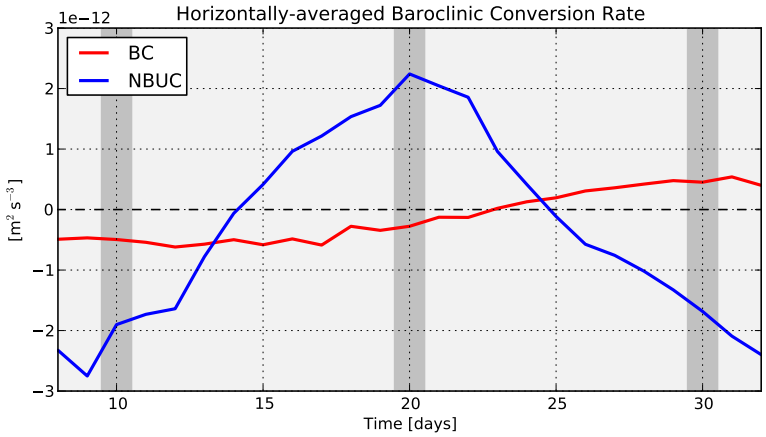

Figure 2.30: Horizontally-avereged baroclinic conversion rate (EC) at the surface (BC) and 400 m (NBUC) between days 10 and 30 of the simulation. The gray shades represents the days that are shown in Figure 2.29. Negative values of EC are merely mathematical results, they have no physical meaning.

between days 20 and 30, which is exactly the time interval between a no-eddy field (Figure 2.29b) and fully developed IE and RCE (Figure 2.29c). Note that the moment when BC EC values started to grow, the NBUC EC values were decreasing. That could probably indicate that the underlying dynamics here is similar to the one reported by *Mano et al.* [2009], where there is an upward baroclinic energy transfer propagation in respect to time. In other words, when the baroclinic conversion starts at BC, it vanishes at NBUC levels, probably indicating that the energy is gradually moving upwards in respect to time.

We believe that these evidences support the underlying dynamical mechanism that leads to the formation of anticyclones at the BC domain rather than the cyclones that would be expected from the interaction with topography (leeward eddies, as in *Magaldi et al.* [2008]). Apparently, since the NBUC is stronger, thicker, and transports more water, it is the first to meander and exhibit baroclinic instability triggering eddies. And finally, in an interval of approximately 10 days, the surface BC responds to it, developing its eddies in the same direction of the NBUC ones. The higher amount of available potential energy at NBUC levels compared to BC levels apparently allows for it to influence the rotation direction preference of the eddies just above, in a baroclinic instability framework.

2.6 Summary and Discussion

Our results show that the main realistic mesoscale features occurring in the eddy-rich vicinities of the BC site of origin can be successfully reproduced by the dynamical interaction between parameterized versions of the mean currents and local topography. A primitive equation ocean model is initialized by feature-modeled velocity fields (CONTROL Experiment), with no atmospheric forcing and no effects of remote dynamics, and the solution compares well with recent *in situ* observations. The three noticeable anticyclones (IE, RCE and AE) described by *Soutelino et al.* [2011] (Chapter 1) were successfully reproduced in terms of their spatial scales, velocity magnitudes and steady or recurrent behavior. All three anticyclones were also observed in the recent analysis of *Arruda et al.* [subm]. The evidences found here suggests stationarity of these anticyclones in the EBRA region.

The cyclonic VE was also successfully generated during CONTROL experiment, with a primarily eastward translational behavior similar to one of the modes proposed by *Campos* [2006] and *Arruda et al.* [subm]. Both *Campos* [2006] (through numerical modeling) and *Arruda et al.* [subm] (satellite-derived altimetry and numerical modeling) reported a translational mode of the VE where it crosses the VTR and propagates northward. *Arruda et al.* [subm] discussed about two possible mechanisms to explain such propagation. One of them is the northward advection of the eddy being caused by the NBUC flow in deeper levels. Since all three anticyclones were also recurrently observed on the recent results of *Arruda et al.* [subm], they argue that another possible mechanism is that the VE is being advected by the offshore side of these eddy features. They used the Okubo-Weiss parameter to *follow* the VE in different northward propagation events. In one of these events, in *Arruda et al.* [subm]-Figures 13-14, the authors reported that the VE propagates just offshore of AE, forming a dipole as it moves close to it, and continues its northward translation. In the present study, the absence of events of northward translation may be explained by the short duration of the time integration.

A set of sensitivity numerical experiments was designed to test different mechanisms (control by either shear or topography) to the anticyclones formation. Results show that both BC-NBUC vertical shear and local topography are both necessary and

sufficient to form the supposedly steady anticlockwise eddies. Each one of these mechanisms were isolated (experiments S1 and S2) and no anticyclones were formed. The BC-topography interaction (S2) was able to trigger cyclonic eddies in the lee of topographic promontories, but no anticyclones were noted. On the other hand, the BC-NBUC interaction over flat bottom (S1) did not generate eddies. It is clear from these two sensitivity experiments that both mechanisms are necessary for the observed eddy formation north of 20°S.

The formation of leeward eddies has been widely reported in the literature. The southward BC flow potentially generates leeward cyclones on the regional EBRA obstacles. On the other hand, the northward NBUC flow in deeper levels going against the same obstacles, potentially leads to leeward anticyclones. So, after performing energy conversion analysis in a QG baroclinic instability framework, we speculate that BC and NBUC are competing to form eddies with different rotation directions and since the NBUC flow is substantially stronger, it is prone to baroclinic instability before the BC is, 10 days later to be more precise, considering the analysis done for the first 30 days of simulation. In other words, since BC is weak and shallow, the surface flow end up being substantially influenced by the NBUC behavior.

We suggest as future work the addition of new sensitivity experiments changing both BC and NBUC transports observing the type of eddies that are generated, accompanied by energy conversion analysis as the one performed here. Studies like this could be useful in the sense that there is possibly annual and inter-annual variability on these WBCs strength and different ratios of BC/NBUC transports could lead to different mesoscale scenarios. A possible implication of this is that the presence of cyclones or anticyclones could lead to different patterns of deep ocean shelf-deep ocean exchanges in the area.

Chapter 3

Final Remarks

3.1 Conclusions

This dissertation goal was to investigate the mesoscale dynamics associated with the South Equatorial Current (SEC) bifurcation and the origin of the Brazil Current (BC), the western boundary current that closes the South Atlantic Subtropical Gyre. There were two distinct chapters addressing the problem through different approaches. Chapter 1 presented a descriptive perspective of the region of interest, creating the basis for a process-study dynamical analysis in Chapter 2.

In Chapter 1, the availability of unique and not yet analyzed *in situ* synoptic datasets, made possible the first observational regional description of the near-surface circulation in the region that encompasses the BC site of origin (10°S-20°S). We questioned the traditional description of SEC bifurcation and BC flow at Brazilian eastern portion. Our findings regarding the regional mesoscale patterns showed a very weak, shallow and disorganized flow for the BC, as opposed to what was previously thought. Intense eddy activity observed in three different synoptic datasets, altimetry records and global model outputs, suggested that there is not a continuous BC in the vicinities of its site of origin. Furthermore, the recurrence of three large anticyclones apparently trapped inside topographic embayments, leaded to speculations regarding flow stationarity, which served as motivation to the analysis carried in Chapter 2.

In a consolidated idea of the flow in the BC site of origin being dominated by eddies, specially regarding stationarity or recurrence of large anticyclonic structures men-

tioned above, lies the motivation of an investigation of the physical roles of topography and vertical shear in generating such patter. This is the subject of Chapter 2.

We start with a review of the three-dimensional mean circulation patterns in the region between 10°S-20°S, emphasizing the existence of a unique western boundary undercurrent (the North Brazil Undercurrent - NBUC) flow bellow BC in an opposite direction. The BC and NBUC together characterize an intense vertical shear within the area, which mixed up with the peculiar topography, would potentially be prone to trigger the observed patterns described in Chapter 1. We designed an analytical/numerical process study set of experiments to address the roles of topography and vertical shear in the formation of the observed structures.

Idealized BC, NBUC and SEC jets were parameterized based on previous research to serve as initial conditions to regional numerical experiments combined in three different scenarios. The parameterized system aimed to reproduce previously known characteristics of the different jets, resulting in a 3-D mass conserving SEC bifurcation and western boundary current system. The complete scenario counted on the three jets interacting with realistic topography for one entire year. One sensitivity setup to isolate BC-NBUC shear mechanism was designed through the creation of an idealized bank-free topography. And finally, to isolate topographic forcing, NBUC was removed from the system in a second sensitivity experiment with realistic bathymetry.

The raw examination of the model outputs during the three experiments was somewhat enlightening. The first interesting result was that in the complete idealized setup the model was able to reproduce the features described in Chapter 1 quite well, indicating that the first order dynamical ingredients were taken into account in the idealized design. The second interesting result is that both sensitivity experiments were unable to reproduce the anticyclones, indicating that both topography and vertical shear are necessary in the regional setup. Although the BC solely interaction with topography was enough to trigger mesoscale eddies, those barely resembled the observed structures. That motivated the question of what is physically happening within the BC-NBUC vertical interaction that would lead to the regional setup in the study area.

Therefore, the subject of Section 2.5 was to address the dynamics of the control experiment model outputs in a quasi-geostrophic baroclinic instability framework. The

baroclinic instability hypothesis was raised because of the vertical shear characteristic of the system, and also because it was pointed as an important mechanism for eddy development downstream of BC by previous studies.

Results of previous work studying flow-topography interaction first helped us to justify the formation of cyclones (anticyclones) at the lee of topographic features if we isolate BC (NBUC) jets. That only fails to explain why anticyclones were actually formed up to the surface. The model output showed that anticyclones were first formed in NBUC levels, and that they were only observed in the surface after 10 days. Our baroclinic instability analysis showed that there was energy conversion from the mean flow to the eddy field occurring in different times for the different BC and NBUC vertical domains, considering the first 30 days of simulation, when the jets evolve from stable rectilineous flow to two major anticyclones. First, baroclinic energy conversion occurs at NBUC levels. In about 10 days, this energy flux reaches a maximum and slowly vanishes, being replaced by an energy conversion in BC vertical domain, exactly when the anticyclones started to appear at the surface.

In order to enunciate a conclusion to this work, we will use two statements to answer the questions posed in Chapters 1 and 2 of this dissertation:

- ✓ The near-surface flow at the Brazil Current site of origin (10°S-20°S) is recurrently dominated by anticyclonic mesoscale eddies.
- ✓ Regionally speaking the complex topography and the interaction between Brazil Current and North Brazil Undercurrent are both essential to explain the mesoscale patterns in the near-surface flow at the Brazil Current site of origin. Geophysical baroclinic instability appears to be playing a key role in the eddy formation.

3.2 Future Work

The first important recommendation that would derive from this work is that the Brazil Current, regarding the present study area, can hardly be compared to western boundary currents like the Gulf Stream, Kuroshio and Agulhas Current. The BC has thickness, velocities and transports one order of magnitude smaller than its world

counterparts. While that was already known by previous research, this work brought new *in situ* data to confirm several speculations about BC thickness and strength near its site of origin.

Although the analyzed datasets were important to our findings, there is still a lot of open questions regarding spatial and temporal variability of the mesoscale activity that could not be addressed because of the *snapshot* nature of them. It is highly recommended that moored velocity sensors are deployed in the region for longer time scales, in order to make possible a thorough understanding of the flow in such key region for inter-hemisphere exchanges.

Regarding the modeling part of this work, despite all the disadvantages of the idealized approach, we believe it makes a strong argument about the importance of the North Brazil Undercurrent flow to the regional patterns of the region. Modeling efforts associated with nowcast and forecast should never underestimate its importance. We suggest that to improve the quality of realistic numerical modeling in the region, one would make sure to use the best representation of this undercurrent in the initialization and open boundary condition prescription.

Our analysis also suggests that ratios between BC-NBUC transports different than the one used here would probably lead to different mesoscale scenarios. Therefore, we suggest new sensitivity experiments changing the strengths of the FMs by seasons. Cause-effect relations could be established comparing different scenarios of SEC, BC and NBUC strengths and the resulting mesoscale patterns in the area, as it is known that there are temporal variability scales associated with these jets strengths. Also, the impinging Agulhas Rings have certainly an effect regionally, and its physics could be extensively explored using available global models and altimetry records.

Bibliography

Arruda, W. Z., E. J. D. Campos, R. G. Soutelino, & I. C. A. Silveira, subm: Events of equatorward translation of the Vitoria Eddy. *Cont. Shelf Res.*, *?(?)*, ?

Biastoch, A. & W. Krauss, 1999: The Role of Mesoscale Eddies in the Source Regions of the Agulhas Current. *J. Phys. Oceanogr.*, *29(9)*, 2303–2317.

Böebel, O., R. E. Davis, M. Ollitraut, R. G. Peterson, P. L. Richard, C. Schmid, & W. Zenk, 1999: The intermediate depth circulation of the Western South Atlantic. *Geophys. Res. Lett.*, *26(21)*, 3329–3332.

Boyer, T., S. Levitus, H. Garcia, R. A. Locarnini, C. Stephens, & J. Antonov, 2005: Objective analyses of annual, seasonal, and monthly temperature and salinity for the world ocean on a 0.25 degrees grid. *Int. J. Climatol.*, *25(7)*, 931–945.

Bretherton, F. P., E. D. Russ, & C. B. A. Fandry, 1976: Technique for Objetive Analysis and design of oceanographic experiments applied to MODE-73. *Deep-Sea Res.*, *23(7)*, 559–582.

Calado, L., A. Gangopadhyay, & I. C. A. Silveira, 2008: Feature-oriented regional modeling and simulations (FORMS) for the western South Atlantic: Southeastern Brazil region. *Ocean Modell.*, *25(1-2)*, 48–64.

Calado, L., I. C. A. Silveira, A. Gangopadhyay, & B. M. Castro, 2010: Eddy-induced upwelling off Cape São Tomé (22°S, Brazil). *Cont. Shelf Res.*, *30*, 1181–1188.

Campos, E., 2006: Equatorward translation of the Vitoria Eddy in a numerical simulation. *Geophys. Res. Lett.*, *33*, L22.607.

Cirano, M., M. M. Mata, E. J. D. Campos, & Deiró, 2006: A circulação oceânica em larga-escala na região oeste do Atlântico Sul com base no modelo de circulação global OCCAM. *Rev. Bras. Geofis.*, *24(2)*, 209–230.

Clarke, R. A., H. W. Hill, R. F. Reiniger, & B. A. Warren, 1980: Current System South and East of the Grand Banks of Newfoundland. *J. Phys. Oceanogr.*, *10(1)*, 25–65.

Cronin, M. & R. Watts, 1996: Eddy-mean flow interaction in the Gulf Stream at 68 °W. Part I: Eddy energetics. *J. Phys. Oceanogr.*, *26*, 2107–2131.

Cummings, J., C. Szczechowski, & M. Carnes, 1997: Global and regional ocean thermal analysis systems. *Mar. Technol. Soc J.*, *31(6375)*.

Dengler, M., F. Schott, C. Eden, P. Brandt, J. Fischer, & R. J. Zantopp, 2004: Break-up of the Atlantic deep western boundary current into eddies at 8°S. *Nature*, *432(7020)*, 1018–1020.

Evans, D. & S. R. Signorini, 1985: Vertical structure of the Brazil Current. *Nature*, *315*, 48–50.

Evans, D., S. R. Signorini, & L. Miranda, 1983: A note on the transport of the Brazil Current. *J. Phys. Oceanogr.*, *13(9)*, 1732–1738.

Fernandes, F. P. A., 2007: Modelos Teóicos Paraméricos do Sistema Corrente do Brasil. Dissertação de Mestrado, Universidade de São Paulo, São Paulo, 66 pp.

Firing, E., J. Ranada, & P. Caldwell, 1995: Processing ADCP data with the CODAS software system version 3.1. Joint Inst. for Mar. and Atmos., Res./NODC, Univ. of Hawaii at Manoa, Honolulu.

Fox, D., M. Carnes, & J. Mitchell, 1992: Characterizing major frontal systems, a now-cast/forecast system for Northwest Atlantic. *5(1)*, 49–53.

Francisco, C. P. F., I. C. A. Silveira, & E. J. D. Campos, 2011: Dynamics of the Brazil-Malvinas confluence: Energy conversions. *J. Phys. Conf. Ser*, *285(2011)*, 012.045.

Gangopadhyay, A. & A. Robinson, 2002: Feature-oriented regional modeling of oceanic fronts. *Dyn. Atmos. Oceans*, *36(1-3)*, 201–232.

Gangopadhyay, A., A. Robinson, & H. Arango, 1997: Circulation and dynamics of the western North Atlantic. I: Multiscale feature models. *J. Atmos. Ocean. Tech.*, *14(6)*, 1314–1332.

Gangopadhyay, A., A. Robinson, P. Haley, W. Leslie, C. Lozano, J. Bisagni, & Z. Yu, 2003: Feature oriented regional modeling and simulation in the Gulf of Maine and Georges Bank. *Cont. Shelf Res.*, *23(3-4)*, 317–353.

Haidvogel, D., H. Arango, K. Hedström, A. Beckmann, P. Malanotte-Rizzoli, & A. Shchepetkin, 2000: Model evaluation experiments in the North Atlantic basin: simulations in nonlinear terrain-following coordinates. *Dyn. Atmos. Oceans*, *32(3-4)*, 239–281.

Hurlburt, H., A. Wallcraft, S. J. W., P. Hogan, & E. Metzger, 1992: Dynamics of the Kuroshio/Oyashio current system using eddy-resolving models of the North Pacific ocean. *J. Geophys. Res.*, *101(C1)*, 941–976.

Joyce, T. M., 1989: On In Situ "Calibration" of Shipboard ADCPs. *J. Atmos. Oceanic Technol.*, *6(1)*, 169–172.

Large, W., J. McWilliams, & S. Doney, 1994: Oceanic vertical mixing: A review and a model with a nonlocal boundary layer parameterization. *Rev. Geophys.*, *32(4)*, 363–403.

Lozano, C. J., A. R. Robinson, H. G. Arango, A. Gangopadhyay, Q. Sloan, P. J. H. Jr., L. A. Anderson, & W. G. Leslie, 1996: An interdisciplinary ocean prediction system: Assimilation strategies ana structured data models. In P. Malanotte-Rizzoli, editor, Modern Approaches to Data Assimilation in Ocean Modeling, volume 61 de *Elsevier Oceanography Series*. Elsevier, 413–452.

Magaldi, M. G., T. M. Özgökmen, A. Griffa, E. P. Chassignet, M. Iskandarani, & H. Peters, 2008: Turbulent flow regimes behind a coastal cape in a stratified and rotating environment. *Ocean Modell.*, *25*, 65–82.

Mano, M. F., A. M. Paiva, A. R. Torres, & A. L. G. A. Coutinho, 2009: Energy Flux to a Cyclonic Eddy off Cabo Frio, Brazil. *J. Phys. Oceanogr.*, *39(11)*, 2999–3010.

Marchesiello, P., J. C. McWilliams, & A. Shchepetkin, 2001: Open boundary conditions for long-term integration of regional oceanic models. *Ocean Modell.*, *3(1-2)*, 1 – 20.

Miranda, L. B. & B. M. Castro, 1981: Geostrophic flow conditions at 19° S. *Ciência Interamericana*, *22(1-2)*, 44–48.

Pedlosky, J., 1987: *Geophysical fluid dynamics*. Springer, New York, 728 pp.

Peliz, A., J. Dubert, D. B. Haidvogel, & B. Le Cann, 2003: Generation and unstable evolution of a density-driven Eastern Poleward Current: The Iberian Poleward Current. *J. Geophys. Res.*, *108(C8)*, 3268.

Peterson, R. J. & L. Stramma, 1991: Upper level circulation in the South Atlantic ocean. *Prog. Oceanog.*, *26(1)*, 1–73.

Pickard, R. S. & S. S. Lindstrom, 1993: A Comparisom of Techniques for Referencing Geostrophic Velocities. *JAOT*, *11*, 814–824.

Pollard, R. & J. Read, 1989: A Method for Calibrating Shipmounted Acoustic Doppler Profilers and limitations of Gyro Compasses. *J. Atmos. Oceanic Technol.*, *6(6)*, 859–865.

Pond, S. & G. L. Pickard, 1983: *Introductory dynamical oceanography*. Butterworth-Heinemann, Oxford, 349 pp.

Reid, J. L., 1989: On the total geostrophic circulation of the South Atlantic Ocean: Flow patterns, tracers and transports. *Prog. Oceanog.*, *23(3)*, 149–244.

Rio, M. H., P. Schaeffer, F. Hernandez, & J. M. Lemoine, 2005: The estimation of the ocean mean dynamic topography through the combination of altimetric data, in situ measurements and GRACE geoid: From global to regional studies. *GOCINA Workshop*, GOCINA Projec, Eur. Union, Luxembourg.

Robinson, A. & S. Glen, 1999: Adaptive sampling for ocean forecasting. *Nav. Res. Rev.*, *51(2)*, 28–38.

Robinson, A., M. Spall, & N. Pinardi, 1988: Gulf Stream simulations and the dynamics of ring and meander processes. *J. Phys. Oceanogr.*, *18(12)*, 1811–1854.

Robinson, A., M. Spall, L. Walstad, & W. Leslie, 1989: Data assimilation and dynamical interpolation in Gulfcasting experiments. *Dyn. Atmos. Oceans*, *13(3-4)*, 301–316.

Rodrigues, R. R., L. M. Rothstein, & M. Wimbush, 2007: Seasonal Variability of the South Equatorial Current Bifurcation in the Atlantic Ocean: A Numerical Study. *J. Phys. Oceanogr.*, *37(1)*, 16–30.

Rowley, C., 1996: A modeling study of the North Atlantic Current. Tese de Doutorado, Grad. School. of Oceanog., University of Rhode Island, Narragansett, Rhode Island, USA, 162p pp.

Schmid, C., H. Schäfer, G. Podestá, & W. Zenk, 1995: The Vitória Eddy and its relation to the Brazil Current. *J. Phys. Oceanogr.*, *25*, 2532.

Schmid, C., G. Siedler, & W. Zenk, 2000: Dynamics of the Intermediate Water in the Subtropical South Atlantic. *J. Phys. Oceanogr.*, *30*, 3191–3211.

Schmidt, A., W. Belo, & J. Lima, 2007: Modelo paramétrico analítico para a estrutura de velocidade do sistema Corrente do Brasil. *Rev. Bras. Geofis.*, *25(1)*, 75–91.

Schott, F. A., M. Dengler, R. Zantopp, L. Stramma, J. Fisher, & P. Brandt, 2005: The shallow and deep western boundary current circulation of South Atlantic at 5°S - 11°S. *J. Phys. Oceanogr.*, *35(11)*, 2031–2053.

Schouten, M. W., W. P. M. Ruijter, P. J. Leeuwen, & H. Ridderinkhof, 2003: Eddies and variability in the Mozambique Channel. *Deep-Sea Res.*, *50(12-13)*, 1987 – 2003.

Shchepetkin, A. & J. McWillians, 2005: The Regional Ocean Modeling System (ROMS): a split-explicit, free-surface, topography following coordinates ocean model. *Ocean Modell.*, *9(4)*, 347–404.

Silva, M., M. Araujo, J. Servain, P. Penven, & C. A. D. Lentini, 2009: High-resolution regional ocean dynamics simulation in the southwestern tropical Atlantic. *Ocean Modell.*, *30(4)*, 256–269.

Silveira, I., J. Lima, A. Schmidt, W. Ceccopieri, A. Sartori, C. Franscisco, & R. Fontes, 2008: Is the meander growth in the Brazil Current system off Southeast Brazil due to baroclinic instability? *Dyn. Atmos. Oceans*, *45*, 187–207.

Silveira, I. C. A., W. S. Brown, & G. R. Flierl, 2000a: Dynamics of the North Brazil Current retroflection from the WESTRAX observations. *J. Geophys. Res.*, *105(C12)*, 28.559–28.583.

Silveira, I. C. A., L. Calado, B. M. Castro, M. Cirano, J. A. M. Lima, & A. S. Mascarenhas, 2004: On the baroclinic structure of the Brazil Current-Intermediate Western Boundary Current System. *Geophys. Res. Lett.*, *31(14)*, L14.308.

Silveira, I. C. A., L. B. Miranda, & W. S. Brown, 1994: On the origins of the North Brazil Current. *J. Geophys. Res.*, *99(C11)*, 22.501–22.512.

Silveira, I. C. A., A. C. K. Schmidt, E. J. D. Campos, S. S. Godoi, & Y. Ikeda, 2000b: A Corrente do Brasil ao largo da costa leste brasileira. *R. bras. Oceanogr.*, *48(2)*, 171–183.

Soutelino, R. G., A. Gangopadhyay, & I. C. A. Silveira, subm: The roles of vertical shear and topography on the eddy formation near the site of origin of the Brazil Current. *Cont. Shelf Res.*, *?(?)*, ?

Soutelino, R. G., I. C. A. Silveira, A. Gangopadhyay, & J. A. Miranda, 2011: Is the Brazil Current eddy-dominated to the north of 20°S? *Geophys. Res. Lett.*, *38(3)*, L03.607.

Spall, M. A. & A. R. Robinson, 1990: Regional primitive equation studies of the Gulf Stream meander and ring formation region. *J. Phys. Oceanogr.*, *20(7)*, 985–1016.

Stramma, L., 1991: Geostrophic Transport of the South Equatorial Current in the Atlantic. *J. Mar. Res.*, *49(2)*, 281–294.

Stramma, L. & M. England, 1999: On the water masses and mean circulation of the South Atlantic Ocean. *J. Geophys. Res.*, *104(C9)*, 20.863–20.883.

Stramma, L., J. Fischer, & J. Reppin, 1995: The North Brazil Undercurrent. *Deep Sea Res. Part I*, *42(5)*, 773–795.

Stramma, L., Y. Ikeda, & R. G. Peterson, 1990: Geostrophic transport in the Brazil Current north of 20°S. *Deep-Sea Res. Part A*, *37(12)*, 1875–1886.

Stramma, L. & F. Schott, 1999: The mean flow field of the tropical Atlantic Ocean. *Deep-Sea Res.*, *46(1)*, 279–303.

Sutton, P. J. H. & T. K. Chereskin, 2002: Absolute geostrophic currents in the East Australian Auckland Current region. *NZJMFWR*, *36*, 751–762.

Verron, J., P. A. Davies, & J. M. Dakin, 1991: Quasigeostrophic flow past a cape in a homogeneous fluid. *Fluid Dynamics Research*, *7*, 1–21.

Webb, D. J., 2000: Evidence for Shallow Zonal Jets in the South Equatorial Current Region of the Southwest Pacific. *J. Phys. Oceanogr.*, *30(4)*, 706–720.

Webb, D. J., B. A. Cuevas, & A. C. Coward, 1998: The first main run of the occam global ocean model. Relatório técnico, Southampton Oceanographic Centre.

Zemba, J. C., 1991: The structure and transport of the Brazil Current between 27° and 36° South. Tese de Doutorado, Massachusetts Institute of Technology and Woods Hole Oceanographic Institution, Massachusetts, 160 pp.